

AD-A096 441 MASSACHUSETTS UNIV AMHERST ASTRONOMY RESEARCH FACILITY F/G 7/4
HIGH-RESOLUTION SPECTRAL MEASUREMENT OF HIGH TEMPERATURE CO2 AN--ETC(U)
DEC 80 H SAKAI AFOSR-78-3702
UNCLASSIFIED UMASS-ARF-80-313 AFOSR-TR-81-0146 NL

for
R-44

END
DATE
FILED
4-11-81
DTIC

AFOSR-TR-81-0146

LEVEL II

12

HIGH-RESOLUTION SPECTRAL MEASUREMENT OF HIGH TEMPERATURE CO₂ AND H₂O

AD A 096441

Hajime Sakai

Astronomy Research Facility
University of Massachusetts
Amherst MA 01003

2 DTIC
ELECTRONIC
MAR 17 1981

December 1980

Final Report

01 July 1978 to 30 September 1980

Approved for public release; distribution unlimited.

THIS DOCUMENT IS BEST QUALITY AVAILABLE.
IT IS THE COPY FURNISHED TO DDC/DTIC.
IT IS UNRECOMMENDED THAT YOU MAKE A
COPY OF THIS DOCUMENT IF THE ORIGINAL IS
LEGIBLY READABLE.

AIR FORCE OFFICE OF SCIENTIFIC RESEARCH
Bolling AFB, D.C. 20332

THIS DOCUMENT IS BEST QUALITY AVAILABLE.
IT IS THE COPY FURNISHED TO DDC/DTIC.
IT IS UNRECOMMENDED THAT YOU MAKE A
COPY OF THIS DOCUMENT IF THE ORIGINAL IS
LEGIBLY READABLE.

81316004

DDC FILE COPY

DISCLAIMER NOTICE

**THIS DOCUMENT IS BEST QUALITY
PRACTICABLE. THE COPY FURNISHED
TO DTIC CONTAINED A SIGNIFICANT
NUMBER OF PAGES WHICH DO NOT
REPRODUCE LEGIBLY.**

UNCLASSIFIED

SECURITY CLASSIFICATION OF THIS PAGE (When Data Entered)

REPORT DOCUMENTATION PAGE		READ INSTRUCTIONS BEFORE COMPLETING FORM
1. REPORT NUMBER AFOSR TR-81-0146	2. GOVT ACCESSION NO. AD-A096 441	3. RECIPIENT'S CATALOG NUMBER
4. TITLE (and Subtitle) HIGH-RESOLUTION SPECTRAL MEASUREMENT OF HIGH TEMPERATURE CO₂ AND H₂O	5. TYPE OF REPORT & PERIOD COVERED Final 01 Jul 78 - 30 Sep 80	
7. AUTHOR(s) Hajime Sakai	6. PERFORMING ORG. REPORT NUMBER UMASS-ARF-80-313	
9. PERFORMING ORGANIZATION NAME AND ADDRESS Astronomy Research Facility University of Massachusetts Amherst MA 01003	10. PROGRAM ELEMENT, PROJECT, TASK AREA & WORK UNIT NUMBERS 61102F 2301/A1	
11. CONTROLLING OFFICE NAME AND ADDRESS Air Force Office of Scientific Research INP Bolling AFB, D.C. 20332	12. REPORT DATE Dec 1980	
14. MONITORING AGENCY NAME & ADDRESS (if different from Controlling Office)	13. NUMBER OF PAGES 77	
16. DISTRIBUTION STATEMENT (of this Report)	15. SECURITY CLASS. (of this report) Unclassified	
17. DISTRIBUTION STATEMENT (of the abstract entered in Block 20, if different from Report)	15a. DECLASSIFICATION/DOWNGRADING SCHEDULE	
18. SUPPLEMENTARY NOTES		
19. KEY WORDS (Continue on reverse side if necessary and identify by block number) Infrared spectroscopy Absorption H ₂ O	CO ₂ High temperature absorption <i>3150 + 0.848, 3117, 3081, 3050, 3030, 3000, 2980, 2960, 2940, 2920, 2900, 2880, 2860, 2840, 2820, 2800, 2780, 2760, 2740, 2720, 2700, 2680, 2660, 2640, 2620, 2600, 2580, 2560, 2540, 2520, 2500, 2480, 2460, 2440, 2420, 2400, 2380, 2360, 2340, 2320, 2300, 2280, 2260, 2240, 2220, 2200, 2180, 2160, 2140, 2120, 2100, 2080, 2060, 2040, 2020, 2000, 1980, 1960, 1940, 1920, 1900, 1880, 1860, 1840, 1820, 1800, 1780, 1760, 1740, 1720, 1700, 1680, 1660, 1640, 1620, 1600, 1580, 1560, 1540, 1520, 1500, 1480, 1460, 1440, 1420, 1400, 1380, 1360, 1340, 1320, 1300, 1280, 1260, 1240, 1220, 1200, 1180, 1160, 1140, 1120, 1100, 1080, 1060, 1040, 1020, 1000, 980, 960, 940, 920, 900, 880, 860, 840, 820, 800, 780, 760, 740, 720, 700, 680, 660, 640, 620, 600, 580, 560, 540, 520, 500, 480, 460, 440, 420, 400, 380, 360, 340, 320, 300, 280, 260, 240, 220, 200, 180, 160, 140, 120, 100, 80, 60, 40, 20, 10, 5, 1</i>	
20. ABSTRACT (Continue on reverse side if necessary and identify by block number) <i>This report describes results obtained in a High-Resolution Spectroscopic Study conducted on the absorption of both CO₂ and H₂O at temperatures up to 800K. An absorption cell which gave a satisfactory performance up to 1000K is described. Approximately 75% of the CO₂ lines observed in the 2400-2100 cm⁻¹ region at 800K are identified. The H₂O data in the 1600-1200 cm⁻¹ region are analyzed for the line assignment, the transition frequency, and the strength.</i>		

SECURITY CLASSIFICATION OF THIS PAGE(When Data Entered)

A large, empty rectangular box with a black border, occupying most of the page below the classification header. It is used to redact sensitive information.

SECURITY CLASSIFICATION OF THIS PAGE(When Data Entered)

Accession For
 X
 AIS GRA&I
 DTIC TAB
 Unannounced
 Justification

By _____
 Distr. _____

Available by Code(s)
 _____ and/or
Dist. _____

A 23 MN

HIGH-RESOLUTION SPECTRAL MEASUREMENT OF HIGH TEMPERATURE CO_2 AND H_2O

Introduction

Both CO_2 and H_2O molecules are a major constituent which critically controls the infrared radiative transfer in the telluric atmosphere. Their absorption bands are distributed over a wide spectral range, extending from the far end of the infrared region to the near end. They have been extensively studied since infrared spectroscopy technology came into existence. Nonetheless, these studies did not provide complete knowledge of the infrared absorption of these two molecules. In particular, our understanding of their absorption at high temperature was rather incomplete. The bands observable at room temperature are restricted to those transitions which originate from a lower state of a relatively small excitation energy, typically from a vibrational-rotational energy below 2000 cm^{-1} . Transitions would be weak at room temperature if their lower states are insufficiently populated at that temperature. They cannot be studied well even if an extremely long absorption path is formed for their measurement. They are for most cases difficult to observe at room temperature, no matter how long the absorption path is extended. They are the transitions which originate from a lower state of high vibrational-rotational energy. They become observable when the gas temperature is raised to increase their population density to a sufficient level. These transitions, generally referred to as the hot bands, were poorly known because very few studies were conducted on them. Various experimental

imposed a major obstacle for pursuing the study of the hot bands. The original AFGL compilation of the atmospheric line parameters was assembled primarily for applications intended to room temperature calculation. The basic line data were derived from the room temperature data. Consequently, the accuracy which the data provided was unsuitable for the spectral synthesis calculation for high temperature. The line parameters compiled for the hot bands of these molecules do not provide an accuracy sufficient for their extrapolation to high temperature. The present experimental study was intended to solve this difficulty by measuring the absorption of these molecules at elevated temperature and to improve their line parameters to such a level that they can produce a satisfactory result for the spectral synthesis at high temperatures.

The excitation which occurs in a heated gas maintains a thermal equilibrium to the molecular system; a population increase at various energy levels is controlled by the Boltzmann factor $e^{-E''/kT}$ where E'' is the vibrational-rotational energy of the state in question. There would be no preferential excitations among various vibrational levels. If two states which belong to two different vibrational states have a similar energy, $E''_1 \approx E''_2$, both states are excited at an equal rate. A marked increase in the observable transitions consequently occurs along two directions as temperature of the molecular system is increased; there is a marked increase in observable vibrational transitions as well as in rotational transitions within the vibrational transition. The spectral structure consequently adds a complexity as the temperature is raised.

An increased complexity in the spectra imposes two problems: one for the spectral resolution requirement, and another for identification of the

spectral transition. The spectra must be observed with a spectral resolution of a highest degree possible. Otherwise, many transitions cannot be resolved. Their observable spectral range broadens as more rotational lines are excited within the vibration band. The problem of spectrometry is, for our case, adequately solved by use of the technique of Fourier spectroscopy. The second problem concerning identification of the observed spectral transition was found more formidable than expected. With anticipated difficulty for the identification effort, the spectral data were taken at a temperature step of 200°K, i.e., at 600°K and at 800°K. We hoped to follow the excitation of the hot bands in the data taken at these temperatures. For the H_2O data, the temperature step taken was adequate, while it was found rather inadequate for the CO_2 data. An increase of the observable CO_2 lines from 600°K to 800°K was overwhelming; at 600°K we were able to make the assignment of the observed CO_2 lines without encountering serious difficulty, while at 800°K the assignment is incomplete even with an automated Loomis-Wood diagram technique which we developed for the purpose of simplifying the identification problem. A detailed description of the 800°K CO_2 data analysis is given later in this report.

Our work performed under this grant may be divided into three categories. The first category, which occupied the first phase of our effort, was to design and to construct the absorption cell which could be operated at elevated temperature. The instrumentation problem we faced during this phase was a question of the stability in the optical path at high temperature operation. With the previously acquired knowledge that the White cell configuration was totally inadequate for high temperature operation, we adopted the Pfund cell configuration, which worked very

well. The multipass optical system was found difficult to make work at high temperature. It worked within a limited temperature range even with the fund cell arrangement. The mirror surface coated with Rh film was adequate for the measurement at 600°K and 800°K. It was found quickly deteriorating as the temperature was raised above 1000°K. A single-pass optical configuration which requires no mirror optics seems the only arrangement which promises a successful operation at temperature above 1000°K. The work on the hot cell was published in Applied Optics. The description of the hot cell work given in this report is actually the published paper.

In parallel with the construction effort for the hot cell, our effort for reassembling the AFGL interferometer was progressed. Upon completion of the interferometer work the second category of our work, the data measurements, commenced during the summer of 1979. The absorption data of both gases were taken at two temperatures, 600°K and 800°K, over a period of approximately ten months. The data were obtained in the spectral range between $1600 \sim 2500 \text{ cm}^{-1}$ because of a limitation imposed by the GeAu detectors which we used for the experiment.

The third category of our work concerned the analysis of the data. Our effort for the CO_2 data taken at 600°K began in the fall of 1979. As mentioned earlier, our analysis effort went smoothly without encountering serious problems. More than 90% of the observed CO_2 lines in $2200 \sim 2400 \text{ cm}^{-1}$ were assigned for the vibrational-rotational transition. When the analysis was switched to the CO_2 data taken at 800°K, the situation was found rather different from what we anticipated from the 600°K data analysis. Approximately 75% of the CO_2 lines observed at this temperature were assigned for their transitions.

The analysis of the CO_2 data reconfirmed our notion that was previously held without a firm supporting evidence. A high accuracy in measurement of the line position provides practically nothing to effect an extrapolation of the rotational transition to those having a higher J value. The vibrational-rotational transitions of a linear polyatomic molecule can be given in the simple expression:

$$\sigma(J) = G + B' J'(J'+1) - D'[J'(J'+1)]^2 + H'[J'(J'+1)]^3 - B'' J''(J''+1) + D''[J''(J''+1)]^2 - H''[J''(J''+1)]^3.$$

It was found that the parameters, B , D , and H , determined from the measurement had a meaningful accuracy only within the measured transition range. They were by no means effective to predict the transitions outside the range. We found that those parameters determined from the data between P(50) to R(50) with an excellent accuracy could predict P(60) to R(60) lines with a disappointing accuracy.

The intensity of the CO_2 lines observed in the data are not determined at the moment. In complex spectral data as ours, a very few observed lines are composed of a single line transition. In dealing with the complex data we must determine the individual line intensity simultaneously for multi-line components. The assignment of the exact position for the component lines plays a crucial importance in the effort. Because of this reason, the identification of all transitions observed in the data takes a prime importance for the data analysis. We need an extended effort for the transition assignment.

The H_2O data contrasted in many ways from the CO_2 data. The H_2O molecule is an asymmetric top rotor; the rotational lines are distributed in a manner not as simple as a linear molecule. Its vibrational frequencies are much larger than those of CO_2 . Even though the H_2O spectrum contains

far less lines than the CO_2 spectrum, its structure is far more complex than the latter. Nonetheless, our analysis effort went well. The identification of the transition, as well as the intensity were determined using the 800°K data.

The obtained results are separately discussed below, one for the CO_2 work and another for the H_2O . Mark Esplin carried out the CO_2 work for his Ph.D. research. The H_2O work was done by Hajime Sakai. The computational effort involved in the data analysis was assisted by Shui-Hua Li. Both the CO_2 and H_2O data measurements were taken by Mark Esplin and William Dalton.

The report consists of three independent parts: the work on the high temperature absorption cell published in Applied Optics, the analysis of the CO_2 data taken at 800°K, and that of the H_2O data taken at the same temperature. The second part is a brief summary of the dissertation that Mark Esplin will complete in the near future. The third part is a pre-print of a paper to be published.

Throughout the entire grant period, we made four presentations at professional meetings: two papers at the Symposium on Molecular Spectroscopy held at the Ohio State University, one at the HIRAD meeting held at the National Bureau of Standards, and one at the OSA Topical Meeting on Spectroscopy in Support of Atmospheric Measurement.

Absorption cell for the infrared spectroscopy of heated gas

William S. Dalton and Hajime Sakai

A Pfund-type absorption cell that exhibits extreme stability at high temperature has been constructed for use with high-resolution Fourier spectroscopy. The cell is currently used to measure the absorption spectra of CO_2 and H_2O gas samples heated to 1300 K. The advantages of the Pfund cell are described with respect to that of the White cell for use in Fourier spectroscopy.

I. Introduction

In the IR region, very few studies have been conducted on the absorption spectroscopy of heated gases. Atmospheric molecules CO_2 and H_2O have been studied up to 1000 K with relatively low spectral resolution.¹ The information obtained by these early high temperature measurements provided a valuable contribution, not only to the understanding of the hot-band transitions in specific but to the molecular physics of these molecules in general. Although the merit of these studies has been well recognized, the difficulties involved in the experiment provided little encouragement for its vigorous pursuit. Prior to recent advances in the IR spectrometric technique, the optical design required for the operation of the absorption cell at a high temperature of ~ 1000 K was rather difficult. To a large extent, this difficulty was solved with our newly constructed cell. In this paper, we will describe our cell, which performs very well for its intended use, i.e., high-resolution absorption spectroscopy of H_2O and CO_2 at high gas temperatures. It was found satisfactory for producing the spectroscopic data taken at a gas temperature of 800 K with a 0.006-cm^{-1} resolution. Our design approach, the testing conducted on various elements, and the spectroscopic data obtained with it will be reported.

II. Cell Design

Long-term stability to maintain a stationary optical output is a prime factor required for the absorption cell, which is used with high-resolution Fourier spectroscopy. An absorption cell operating at a high temperature is subjected to severe mechanical strain. Our preference of the Pfund configuration³ over the White configuration⁴ is based on the required stability. The White configuration, which is designed to provide a flexible optical path by adjusting the mirror alignment, is inherently unstable in a long-term operation. The mirror mounts are necessarily complicated to furnish a certain adjustable setting of the mirrors. They cause a significant drift upon a slow accumulation of the mechanical strain. In the high temperature operation, a build-up of the mechanical strain is more accentuated, as the structural temperature is raised from room temperature to that desired for the operation. We found it almost impossible to design a mirror mount that would meet our requirements. The Pfund configuration, shown in Fig. 1, is much less adaptable than the White configuration in providing a flexible optical path, although it can provide some degree of flexibility. The optical configuration allows no internal adjustment, and the number of passes must be adjusted by means of the external optical scheme. Once the mirrors are properly mounted in the cell, they are held at their position securely. A drift in the optical output results only if the cell body deforms severely. Thus, stability is well furnished in the design. In addition, the stability for maintaining the stationary optical output is further improved by our design, which is to separate the heating element from the absorption cell body. The cell structure is constructed separately and placed in the furnace. The space between the furnace inner wall and

The authors are with University of Massachusetts, Astronomy Research Facility, Amherst, Massachusetts 01003.

Received 12 March 1980.

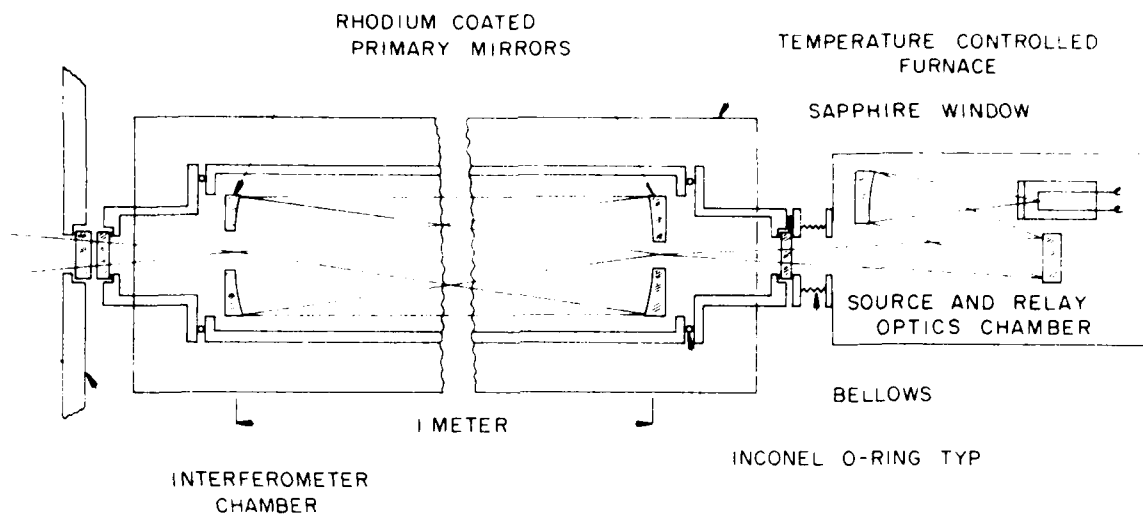


Fig. 1. High temperature absorption cell.

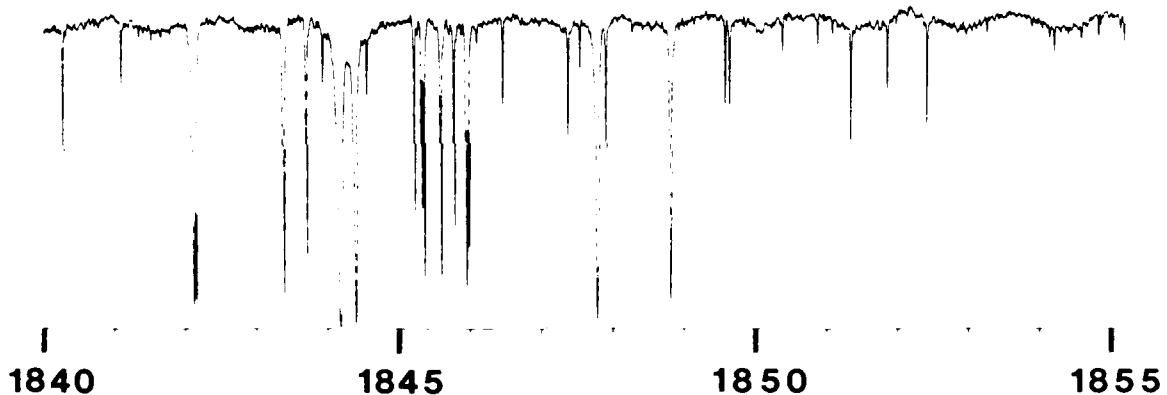


Fig. 2. Spectrum of H_2O taken in the $1840\text{-}1855\text{-cm}^{-1}$ region with 0.006-cm^{-1} resolution, 6-Torr H_2O pressure, and 600-K temperature. The figure shows a short section of the entire data taken in the $1600\text{-}2400\text{-cm}^{-1}$ region.

the cell body provides a thermal cushion. A heat flow between them is smoothed out in this configuration, even if the control circuitry to the furnace for maintaining the operating temperature undergoes on-off cycles rather frequently.

The cell body was constructed of series 310 stainless steel (AISI code), which has a sublimation temperature of $\sim 1650\text{ }^\circ\text{C}$, well above our maximum operating temperature. The material was selected because of its easy machinability and desirable characteristic for welding. It is reasonably stable at high temperature: a low thermal expansion coefficient ($1.4 \times 10^{-5}\text{ cm}^{-1}\text{ }^\circ\text{C}^{-1}$) and an excellent atmospheric resistance to scaling. We

noticed a slightly increased chemical reaction of this stainless steel to H_2O and CO_2 at temperatures $>600\text{ K}$. The gas pressure in the cell gradually decreases at a slow rate, but it does not significantly interfere with the measurements.

The interferometric configuration used in Fourier spectroscopy makes the spectrometric efficiency very high compared with the conventional configuration. We, therefore, can afford some loss in the optical throughput of the hot cell. The optics in the final form was an $f/14$ beam with a mirror separation distance of 1 m, achieving a 3.5 m path between both entrance and exit ends. The mirror substrate was tested for surface

stability with an Rh film coating as well as for a chemical reaction at high temperature operation. We chose clear synthetic fused silica after a series of tests conducted on prepared samples of fused silica, Corning Glass Works premium grade Cervite C101 and General Electric Ultra Low Expansion glass, in a small furnace with temperatures cycling between ambient room temperature and 1300 K. The fused silica and the ULE sample fared well in the test, showing no appreciable deterioration, while the Cervite did not.

The standard coatings for IR mirrors such as Al, Ag, and Au are unusable at the operating temperature required for the measurements. A test was conducted on the effect of the temperature to the reflectivity of rhodium. The reflectivity of a 500-Å thick Rh film deposited on several pieces of polished silica was measured in the 2-6-μm region prior to the heating test. After heating them to 600 K for a period of 24 h, letting them cool, and measuring their reflectivity under identical conditions as those prior to heating, we detected a deterioration of ~10% in reflectivity. The same procedure was followed for temperatures of 900 and 1300 K, and the deterioration in reflectivity was found to be 30 and 70%, respectively. The Rh coating remained attached to the substrate but became discolored at 1300 K. Although this is considered far from an ideal situation, the throughput of our system is more than adequate to make up for the loss. (The deterioration of the mirrors with temperature would be disastrous for a multiple-traversal operation.) Two of these mirrors have been in use ~6 months at 600 K, and we observed about a 10% degradation in signal level, which occurred at the first use of the system.

The mirrors were mounted on a standard 3-point mirror holder with a ceramic fiber backing. The thin section of fiber gave the mirror just enough freedom of movement to prevent cracking. Also, the continuous filament ceramic fiber, brand AB-312 manufactured by the 3M Company, has good chemical resistance and dimensional stability at temperatures >1300 K.

Most of the window crystals transparent in the IR region are not heat resistant. They are so fragile that hard contact to a hot metal frame is unworkable. No technique has been developed for providing a delicate mount for these crystals onto the hot metal structure. The only choice left to us is to mount the window crystal on the lukewarm frame using an O ring or a gasket made of pliant material. Our design places both end sections of the cell outside the furnace. The windows are cooled either by natural convection heat loss or by forced coolant circulation. The window crystals are mounted to the cell body through a silicon O ring, forming a vacuum-tight seal. With the main section of cell being heated at 600 K, the window portion remains at ~330 K. The temperature distribution in the cell is quite uniform with ±2 K over the entire length except in the proximity of ~10 cm to the window where the temperature drops very rapidly. The cell is made of three sections as shown in Fig. 1; both ends of a main central section are connected through a gas-filled Inconel O ring to a short end section on which the window is mounted.

The structure enables us to access the mirror for alignment as well as for replacement purposes. The system has remained tight during the past 6 months of operation.

III. Furnace

The main factor in the consideration to separate the absorption cell and the furnace has been described already. Our design was certainly influenced by a well designed furnace readily available on the commercial market. It is manufactured by the Mellen Company, Webster, New Hampshire. The heat output of the furnace is controlled by thermocouples placed inside the wall of the absorption cell. The cell temperature is controlled within ±2 K over the entire measurement period. This arrangement is convenient in that the cell can be easily accessed for replacement and/or repair. The positional stability of the overall structure is well demonstrated in the data obtained.

IV. Results and Conclusions

Since the absorption cell was completed, we have been vigorously taking the spectroscopic data of heated gas. Figure 2 shows a part of the data taken with H₂O pressure of 6 Torr at 600 K. It is a short portion of the entire spectrum that covered from 1600 to well over 2200 cm⁻¹ with a 0.006-cm⁻¹ spectral resolution. The spectrometry achieved is judged by the quality factor defined by Connes:

$$Q = (s/n) \text{ spectrum} \left(\frac{\text{spectral coverage}}{\text{resolution}} \right).$$

The quality factor of the data shown in Fig. 2 is ~10⁷. The interferogram measurement takes ~10 h to cover the optical path difference of 80 cm.

This research was supported by AFOSR grant 78-3702.

References

1. J. H. Taylor, W. S. Benedict, and J. Strong, *J. Chem. Phys.* **12**, 1884 (1952); Y. Ben Aryeh, *J. Quant. Spectrosc. Radiat. Transfer* **7**, 201 (1967); Shau-Yau Ho, *Infrared Phys.* **14**, 37 (1974).
2. H. Sakai, "High-Resolving Power Fourier Spectroscopy," in *Spectrometric Techniques*, I. G. Vanasse, Ed. (Academic, New York, 1977).
3. The Pfund configuration applied for the high temperature absorption cell was described in J. H. Taylor, Dissertation, Johns Hopkins U., Baltimore (1952).
4. J. U. White, *J. Opt. Soc. Am.* **32**, 285 (1942).
5. P. Connes, in *Proceedings, Asper International Conference on Fourier Spectroscopy*, '67, G. Vanasse, A. T. Stair, and D. Baker, Eds., AFCRL Special Report 114 (1971), p. 121.

II. CO_2

The importance of CO_2 as an atmospheric molecule makes the obtaining of high precision band parameters for a great number of bands a significant contribution to both theoretical and experimental studies of our atmosphere. Very accurate parameters on the (00001-00011)* band of $^{12}\text{C}^{16}\text{O}_2$ have been obtained by Pine and Guelachvili.¹ Their measurement was accomplished by combining two spectra, a room temperature Fourier transform spectrum and a high temperature tunable laser spectrum. There have been numerous measurements of other bands of CO_2 , but they were made either with lower resolution spectrometers, or near room temperature where fewer rotational lines were excited,^{2,3} resulting in a less accurate determination of band parameters. In this work a high resolution Michelson interferometer was coupled with a high temperature absorption cell heated to 800°K to obtain a high resolution (0.007 cm^{-1}), high temperature spectrum of CO_2 in the 4.3 micron region.

The energy of a linear molecule in a given vibrational-rotational state can be represented by

$$E(v, J) = G(v) + B[J(J+1)] - D(v)[J(J+1)]^2 + H(v)[J(J+1)]^3$$

where v is the quantum number associated with vibrational energy, J is the quantum number associated with total angular momentum of the molecule, and $G(v)$, $B(v)$, $D(v)$, and $H(v)$ are the band parameters. The infrared spectrum corresponds to the transitions between different vibrational-rotational states.

The advantages of taking the measurements at an elevated temperature are twofold. First, at the higher temperature more rotational lines are

*For CO_2 there are three fundamental modes of vibration, v_1 , v_2 , and v_3 . Associated with the bending mode, v_2 , is the angular momentum ℓ . The notation used is $v_1 v_2 \ell v_3 r$ where r is the ranking index for a Fermi resonating group.

excited, making it possible to obtain higher precision in the determination of the spectroscopic constants $G(v)$, $B(v)$, $D(v)$, and $H(v)$. Secondly, the higher temperature results in higher vibrational energy levels being excited, making more of the so-called "hot bands" visible.

We used a PDP-8e mini-computer to control the interferometer and to sample the interferogram. The data was taken via magnetic tape to be analyzed using the CDC 6600 computer at the University of Massachusetts in Amherst. The data was first Fourier transformed, the various lines identified, and finally a least-square-fit technique was used to generate new values for the band parameters. Each band was fit independently of the other bands.

Spectra obtained using high resolution Fourier transform spectrometers have an excellent frequency stability over a wide spectral range. There is, however, a small systematic frequency shift introduced into the spectra due to finite detector size.⁴ In principle, this correction can be calculated from the geometry of the interferometer apertures and detectors, but in practice it is usually easier to use an internal frequency standard. Lines due to CO were present in our experimental spectrum. Guelachvili has measured the position of these CO lines with an accuracy of 0.00008 cm^{-1} .⁵ We used these line positions as an internal frequency standard. After this systematic error was removed from our spectra, the standard deviation of the fit between our data and Guelachvili's, on well isolated lines, was about 0.0004 cm^{-1} .

One disadvantage of taking spectral measurements at high temperatures is the difficulty of constructing a high temperature absorption cell that is mechanically stable, and whose structural materials can withstand the high temperature. The absorption cell used in this work has previously been

described in more detail.⁶

Another complication that arises in working with high temperature spectra of CO_2 is the large number of lines present. Tens of overlapping bands, each consisting of hundreds of lines, result in an observed line density of over 20 lines/ cm^{-1} .

The identification was made in one of three ways, depending on how well the band had previously been measured. For well known bands the identification procedure was readily automated. The position and strength of each line was calculated, and then used to locate the line in the experimental spectrum with approximately the right strength that was closest to the calculated position.

For other bands, the positions of lines for low J have been well measured, but not for high J . In this case, the line positions were again calculated and the experimental lines identified, starting at low J and moving up to higher J , until there were not any lines within about 0.02 cm^{-1} of the calculated line. The band was then refit and new constants obtained. The process was iterated until no further extension to higher J was possible.

In some cases the band was so poorly known even at low J that the identification could not be made by taking the experimental line closest to the calculated line position. Another problem arose when certain combinations of merged lines made the extension from low J to higher J impossible. In these two cases, a Loomis-Wood diagram⁷ approach has been extremely helpful in picking out the lines that belong to one band in the presence of lines belonging to other bands. When the differences between a calculated line and all observed lines that are nearby are displayed graphically, it is relatively easy to see the pattern created from a set of lines which have band parameters similar to those used to calculate

the line positions.

After the identification of lines was determined, each band was fit throwing out only the most severely merged lines. Lines for which the difference between the observed and calculated position was less than about 0.005 cm^{-1} were kept in the fit. All lines used in the fit were weighted equally. The bands that were fit are given in Table I, along with the standard deviation, the range of J values used, and the total number of lines used in the fit. The resulting values obtained for $G(v')$, $G(v'')$, $B(v')$, $D(v')$, $H(v'')$, $B(v'')$, $D(v'')$, and $H(v'')$ are tabulated in Table II.

Several constraints were used on the fits. The constants $H(v')$ and $H(v'')$ are given as zero. For bands with l greater than or equal to two, both the C and the D bands were fit together. For bands with l equal to two, the parameters $G(v')$, $G(v'')$, $B(v')$, and $B(v'')$ were held common for both bands, where the parameters $D(v')$, $D(v'')$, $H(v')$, and $H(v'')$ were allowed to be dissimilar for the two bands. For bands with l greater than two, the C and the D bands were fit entirely together, with no distinctions between the two bands.

The difference between the band parameters determined by Guelachvili, and the AFGL line compilation, for the P branch of the 02201-02211 band of $^{12}\text{C}^{16}\text{O}_2$, have been compared to the band parameters as shown in Figure 1. Guelachvili made extremely accurate room temperature measurements (0.0001 cm^{-1}) of the position of lines up to about $J = 46$ of this band, from which he calculated band parameters.⁸ For low J (less than 50), the agreement with this work is excellent, but for high J the difference is large.

The large values of the standard deviations given in Table II, considerably greater than the 0.0001 cm^{-1} for well isolated lines mentioned

earlier, are caused by merging of lines. Most observed lines are merged to some degree. If lines causing merging belong to bands that are not correlated with the band being fit, the effect of the merged lines will be an increase in the random scatter of the fit. It is very rare to have both the position and the spacing between the lines of the band being fit and lines in a merging band close enough that significant correlation occurs. The strongest correlation between bands in the observed spectrum appears to be between C and D bands. For example, the 01101C-01111C and the 01101D-01111D bands have spectroscopic constants just enough different that even though they have the same band origin, $R(105)$ of the C band is merged with $R(106)$ of the D band. At this point in the bands, the difference between the line spacing is only 0.005 cm^{-1} , yet $R(102)$ is not merged with $R(104)$, or $R(107)$ is not merged with $R(108)$. The smallness of the correlation between bands supports the assumption that fitting partly merged lines is valid.

To further insure that the identification and fitting procedure was valid, a synthetic spectrum was calculated and compared to the observed spectrum. The band parameters listed in Table II and the band intensities given in reference 9 were used to create the synthetic spectrum. Bands that resulted in higher absorption in the synthetic than in the observed spectrum were either refit or thrown out entirely.

References

1. A.S. Pine and G. Guelachvili, *J. Mol. Spectrosc.* 79, 84-89 (1980).
2. T.K. McCubbin, J. Pliva, R. Pulfrey, W. Telfair, and T. Todd, *J. Mol. Spectrosc.* 49, 136-156 (1974).
3. A. Baldacci, V.M. Devi, D. Chen, and K.N. Rao, *J. Mol. Spectrosc.* 70, 143-159 (1978).
4. G. Vanasse and H. Sakai, "Fourier Spectroscopy" in Progress in Optics, Vol. VI, ed. E. Wolf, North-Holland, Amsterdam (1967).
5. G. Guelachvili, *J. Mol. Spectrosc.* 75, 251-269 (1979).
6. W.S. Dalton and H. Sakai, *Appl. Opt.* 19, 2413-2415 (1980).
7. G. Herzberg, Spectra of Diatomic Molecules, Second Ed., p. 191, Van Nostrand Reinhold, New York (1950).
8. G. Guelachvili, *J. Mol. Spectrosc.* 79, 72-83 (1980).
9. R.A. McClatchey *et al*, AFCRL Report No. 434, 73-0096, p. 26 (1973).

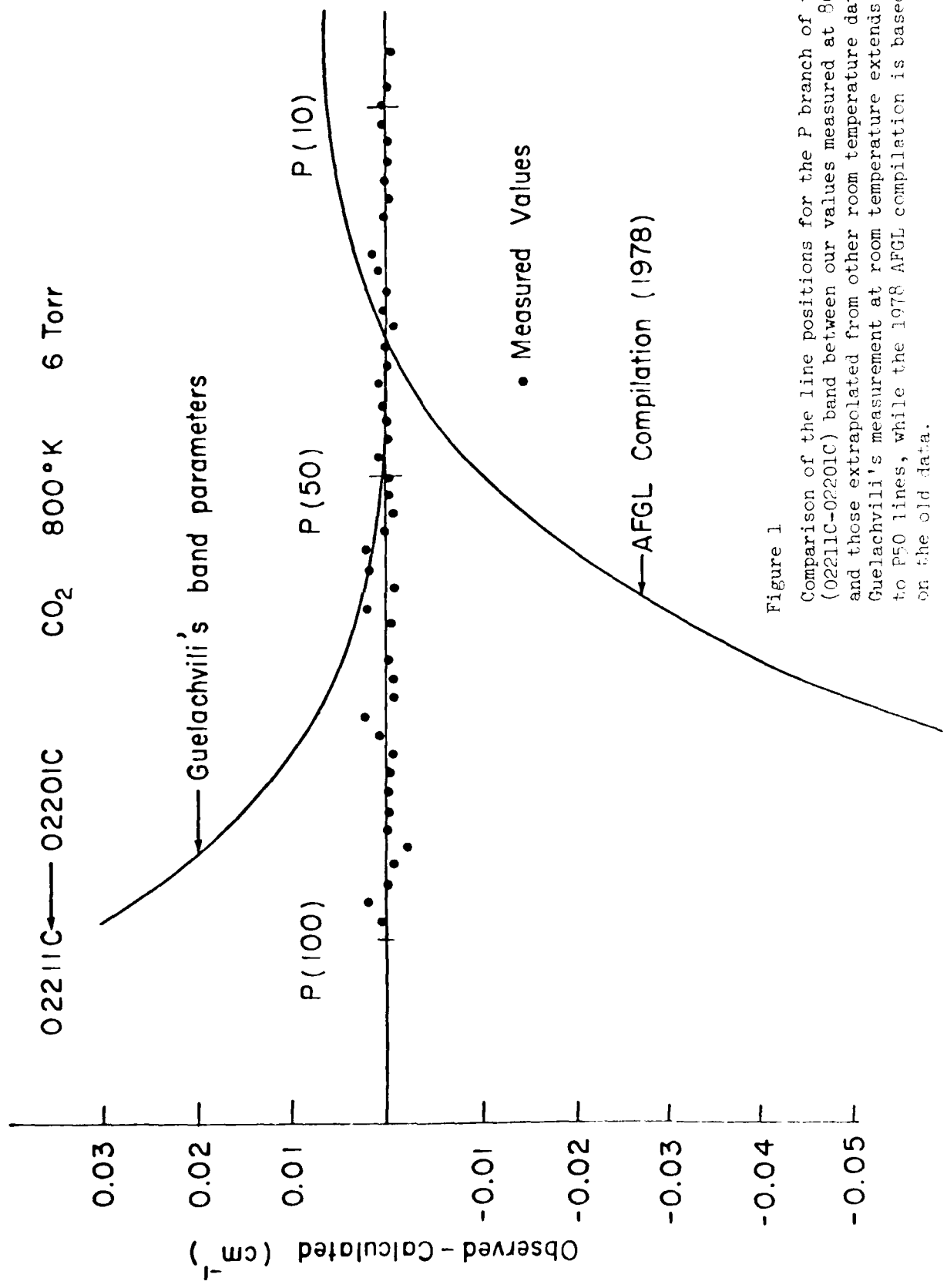


Figure 1

Comparison of the line positions for the P branch of the (02211C-02201C) band between our values measured at 800°K and those extrapolated from other room temperature data. Guelachvili's measurement at room temperature extends up to P50 lines, while the 1978 AFGL compilation is based on the old data.

Table I

The CO₂ bands studied in the present work.

Transition	Isotope	Band Center (cm ⁻¹)	Range of Measurement
0 0 0 1 1	626	2349.1430	P120-R118
0 1 1 1 1 C	626	2336.6330	P107-R109
0 1 1 1 1 D	626	2336.6330	P108-R104
1 0 0 1 2	626	2327.4330	P102-R102
0 2 2 1 1 C	626	2324.1410	P98-R104
0 2 2 1 1 D	626	2324.1410	P105-R107
1 0 0 1 1	626	2326.5980	P104-R104
1 1 1 1 2 C	626	2315.2350	P67-R63
1 1 1 1 2 D	626	2315.2340	P86-R88
0 3 3 1 1	626	2311.6680	P90-R92
1 1 1 1 1 C	626	2313.7720	P89-R87
1 1 1 1 1 D	626	2313.7720	P88-R88
2 0 0 1 3	626	2305.2570	P80-R76
1 2 2 1 2 C	626	2302.9580	P68-R62
1 2 2 1 2 D	626	2302.9580	P67-R67
0 4 4 1 1	626	2299.2140	P82-R83
2 0 0 1 2	626	2306.6900	P86-R56
1 2 2 1 1 C	626	2301.0530	P86-R88
1 2 2 1 1 D	626	2301.0530	P83-R83
0 0 0 2 1	626	2324.1830	P82-R87
2 0 0 1 1	626	2302.5230	P82-R78
0 0 0 1 1	636	2283.4870	P82-R82
0 1 1 1 1 C	636	2271.7590	P71-R61
0 1 1 1 1 D	636	2271.7610	P74-R58
1 0 0 1 2	636	2261.9110	P56-R58
0 2 2 1 1 C	636	2260.0520	P50-R46
0 2 2 1 1 D	636	2260.0520	P53-R51
1 0 0 1 1	636	2262.8460	P54-R48
2 1 1 1 2 C	626	2293.4110	P71-R71
2 1 1 1 3 D	626	2293.6100	P76-R74
0 1 1 2 1 C	626	2311.7030	P90-R80
0 1 1 2 1 D	626	2311.7000	P83-R79
1 0 0 2 2	626	2302.3690	P69-R67
0 2 2 2 1 C	626	2299.2400	P75-R93
0 2 2 2 1 D	626	2299.2380	P78-R80
0 5 5 1 1	626	2286.7770	P64-R66
1 3 3 1 1	626	2288.3900	P65-R63
1 3 3 1 2	626	2290.6800	P73-R66

TABLE II (All are in cm^{-1})

Band	G"	G' - G"	B'	D' $\times 10^7$	H' $\times 10^{-13}$	B"	D"	H" $\times 10^{-4}$
00011	0.000	2349.143	.38713745	1.32514	-.1	.39021480	1.32815	-.1
01111C	01101C	626	667.379	2336.633	.38759128	1.34823	.3	.39063793
01111D	01101D	626	667.379	2336.633	.38818885	1.35624	.2	.39125338
10012	10002	626	1285.409	2327.433	.38750303	1.57182	1.9	.3908172
02211C	02201C	626	1335.129	2324.141	.38863751	1.37657	-2.2	.39166830
02211D	02201D	626	1335.129	2324.141	.38863751	1.38347	.8	.39166830
10011	10001	626	1388.187	2326.598	.38706354	1.14847	2.3	.39016922
03311	03301	626	2003.238	2311.668	.38937836	1.39742	-.4	.39138084
11111C	11101C	626	2076.865	2313.772	.38735962	1.21874	-1.2	.3910322
11111D	11101D	626	2076.865	2313.772	.38822645	1.17343	-2.4	.3913251
00021	00011	626	2349.141	2324.183	.38406499	1.31129	-2.3	.38714060
20013	20003	626	2548.373	2305.257	.38818763	1.79054	3.8	.39110066
12211C	12202C	626	2585.032	2302.958	.38894365	1.35669	0.0	.39193107
12211D	12202D	626	2585.032	2302.958	.38894365	1.48755	0.0	.39193107
20012	20002	626	2671.146	2306.690	.38652310	1.35362	10.6	.38954825
04411	04401	626	2671.690	2299.214	.39010454	1.39091	-1.6	.39307315
12211C	12201C	626	2760.735	2301.053	.388853501	1.34651	-15.0	.39135785
12211D	12201D	626	2760.735	2301.053	.388853501	1.32085	6.6	.39155785
20011	20001	626	2797.154	2302.523	.38747238	.87851	-4.5	.39057680
01121C	01111C	626	3004.016	2311.703	.38456350	1.40044	6.6	.38761095
01121D	01111D	626	3004.016	2311.700	.38512829	1.34645	-1.2	.38818842
13312	13302	626	3240.564	2290.680	.38971034	1.47398	0.0	.39165318
13311	13301	626	3442.256	2288.390	.38924068	1.31704	0.0	.39220963
10022	10012	626	3612.840	2302.369	.38452333	1.66712	17.0	.38718663
02221C	02211C	626	3659.277	2299.240	.38560401	1.32035	5.4	.38863983
02221D	02211D	626	3659.277	2299.238	.38556943	1.28275	-6.1	.38859689
00011	00001	636	0.000	2283.487	.38727283	1.32429	-.2	.39023617
01111C	01101C	636	648.484	2271.759	.38767594	1.29905	-8.8	.39060610
01111D	01101D	636	648.484	2271.761	.38828278	1.31849	-2.6	.39123536
10012	10002	636	1265.820	2261.911	.38803282	1.55644	-9.9	.39091903
02211C	02201C	636	1297.269	2260.052	.38870822	1.58213	0.0	.39162783
02211D	02201D	636	1297.269	2260.052	.38870822	1.37269	0.0	.39162783
10011	10001	636	1370.067	2262.846	.38676005	1.30651	0.0	.38975035

H₂O

The infrared absorption of H₂O is one of the most intensively measured spectroscopic data. Since the infrared spectrometers capable of a spectral resolution exceeding 0.1 cm⁻¹ were developed in the 1950's, the H₂O spectra throughout the entire infrared range were measured with a majority of the lines resolved. Both study efforts, experimental and theoretical, were progressed in parallel with development of the high-resolution infrared spectroscopy. A principal object of the experimental effort was to make a high precision measurement of the transition frequencies, the strengths and the widths, while that of the theoretical effort was to furnish the proper assignment for the observed transitions, as well as the calculated values for the transition parameters in a good agreement with the observed data. By the early 1970's the experimental data were accumulated in a sufficient quantity so that the global compilation of the H₂O line data throughout the infrared spectral region became possible. In 1973, the group headed by the late William S. Benedict accomplished the monumental compilation of the H₂O line data which was a major achievement included in the AFGL atmospheric line listing.¹ With these line data, for the first time in fifty years of infrared spectroscopy, we had access to a global knowledge of the infrared H₂O transitions. Since the early 1970's, infrared spectrometry went through another revolutionary advance. The spectral resolution achieved in the data measurement was improved by one to two orders of a magnitude. The data measurement became very efficient; a high quality spectrum which contains 10⁵ ~ 10⁶ spectral elements was obtained in a routine measurement of several hours duration. The position of the transition lines became known to an accuracy within ±.001 cm⁻¹. Both the advance in spectrometric technique and the extensive compilation of the spectroscopic line data in

turn provided a strong incentive for re-examination of the AFGL H_2O line data compilation. The consequent improvement in the current AFGL compilation was based on a series of theoretical works carried out by Flaud and Camy-Peyrot.² The listed position of the H_2O transitions observable at room temperature gained an accuracy figure better than $\pm 0.01 \text{ cm}^{-1}$.

The transitions observable at room temperature are those which have a lower state energy below 2000 cm^{-1} . The transitions which start from the initial lower state of a higher vibrational-rotational energy are weak at room temperature, because the lower state is insufficiently populated. They become observable as the lower state population is increased by means of thermal excitation. They are commonly called the "hot band" lines because their absorption increases with rising gas temperature. The list of the H_2O energy levels compiled in the work of Flaud and Camy-Peyrot provides an insufficient coverage for the study of the hot band lines. In the past, a majority of the H_2O spectral study was conducted on the absorption data taken at room temperature. A very few studies were made on the high temperature absorption data.³ In $1600 \sim 2000 \text{ cm}^{-1}$, no studies were carried out on the high temperature H_2O absorption. The present experimental study was intended to remove this deficiency and to fill the need for improvement of the hot-band line data in this spectral region by measuring the absorption spectrum of H_2O at elevated temperature.

Experimental

The experimental arrangement for the present study was already described elsewhere. The following description summarizes the information pertinent to the present study. The spectrometer used for the data measurement was a cat's eye type Michelson interferometer designed to measure the interferogram data

using the step-and-integrate scanning mode.⁴ The data were sampled with a multiple of an interference fringe distance by the single mode cw He-Ne laser line at 6329.9A in vacuum. The interferometer was operated in vacuum. The laser line was stabilized by the Lamb dip at the center of the laser transition.⁵ The spectral data was expected to exhibit a downward frequency shift by 0.0020 cm^{-1} in 2000 cm^{-1} region because of a finite aperture size of the detector used.⁶ The parasitic CO lines observable in the data were used as the internal standard for the wavenumber calibration. The measured positions of the CO lines were $.00206 \text{ cm}^{-1}$ in average lower than the values published by Guelachvili.⁷ All of our measured wavenumber figures were accordingly adjusted to include the constant shift of $-.00206 \text{ cm}^{-1}$. The spectral resolution of the data was $.0060 \text{ cm}^{-1}$.

The high temperature absorption cell⁸ was connected to the interferometer optics placed in vacuum via a short air space of approximately .25 cm, which was the only path exposed to the ambient environment. The rest of the optical path connecting the source to the interferometer via the absorption cell was kept in a pressure below 1 torr. The H_2O pressure in the absorption cell was measured by the Baratron pressure gauge.

Absorptance Spectra

The observed data for our study contained a 100% transmittance-level rather non-uniformly varied as a function of the wavenumber. The variation resulted from several factors, the change in the spectral sensitivity of the detector, the spectral transmission characteristics of the bandpass filter, and so forth. The most troublesome background level modulation was caused by the interference of the various optical surfaces through which the infrared beam was transmitted. The H_2O absorptance was determined against the non-uniform 100% transmission level. Various computation logics were

employed to determine the 100% transmittance level in hope for reducing any speculative aspect to a minimum level. In the end, there still existed some degree of speculation in determination of the absorptance, possibly amounting to 5% in average.

Data Analysis

The absorptance spectra thus determined were at first analyzed for the transition frequencies. Since the data points were spaced at a finite resolution interval given by an inverse of twice the maximum optical path difference, smooth contour generated by interpolating these data points was used for the data analysis. The line centers were determined using the first and the second derivative calculated from the interpolated spectral data. The uncertainty in the line center frequency was affected by the noise in the data as well as by the blending of the neighboring lines. The uncertainty figure was larger for the lines which were strongly saturated at the center, even for the case where they were well isolated from their neighbors. The over-all uncertainty figure in the measured transition frequency was a value close to the smallest interval used in the interpolation, 0.0004 cm^{-1} . No special effort was taken to improve the uncertainty figure beyond this limit.

The absorption contour of the molecular transition in the observed spectra is expressed in a good approximation by a convolution integral of the true absorption contour and the impulse response of the instrument, commonly called the instrument function. For the spectrum obtained by using the technique of Fourier spectroscopy, it is more conveniently expressed in a form of the interferogram, defined in the optical path difference scale x , rather than in a form of the spectrum, defined in the wavenumber scale σ . The observed contour $A'(\sigma)$ and the true contour $A(\sigma)$ are

related by

$$\int A'(\sigma) e^{i2\pi\sigma x} d\sigma = \{ \int A(\sigma) e^{i2\pi\sigma x} d\sigma \} T(x), \quad (1)$$

where $T(x)$ is a multiplicative function of a finite extension which is caused by the interferogram data coverage limited to the maximum optical path difference X . The function $T(x)$ takes a special shape dependent on the type of the apodization applied to the spectral data. For our case, it is a triangular function tapered to zero at the maximum path difference X ;

$$T(x) = 1 - \frac{|x|}{X} \quad \text{if } |x| \leq X,$$

$$\text{and} \quad = 0 \quad \text{if } |x| > X. \quad (1)$$

The true absorptance contour of a well-isolated molecular transition line is expressed by

$$A(\sigma) = 1 - \exp [-k(\sigma)] \quad (2)$$

where the function $k(\sigma)$ is called the absorption coefficient defined by the transition strength S per a single molecule in a form

$$\int k(\sigma) d\sigma = SN. \quad (4)$$

In this formulation we assume that the absorption is caused by a uniform column of N total molecules per a unit cross-sectional area. If the thermal equilibrium exists along the absorption path, the strength S is written in a well known formula:

$$S = \frac{8\pi\nu}{3hc} |R|^2 \left(1 - e^{-\frac{h\nu}{kT}}\right) \frac{1}{g} e^{-E''/kT}$$

where ν is the transition frequency in Hz, R is the transition moment, g is the statistical weight of the lower state, and E'' is the lower state energy. The absorption coefficient $k(\sigma)$ takes various shapes subject to the line profile. If we can assume that the collisions from the neighboring molecules dominate the broadening process of the transition line, we can express the absorption coefficient by the Lorentzian profile:

$$k(\sigma) = \frac{S\alpha}{\pi[(\sigma - \sigma_0)^2 + \alpha^2]}, \quad (5)$$

where α is the width and σ_0 is the center frequency of line.

The observed spectrum for most cases contains the lines overlapped by their neighbors. The absorptance contour for the overlapped lines is given by

$$A(\sigma) = 1 - \exp - [\sum_{n=1}^N k_n(\sigma)], \quad (6)$$

where the absorption consists of N lines, and $k_n(\sigma)$ is the absorption coefficient for the n -th line. The data which we deal with in the analysis contain the situations from one extreme to another, i.e., from the case for well isolated lines to the one containing many overlapping lines. Our objective in the spectral analysis is to determine the line parameters of each transition, the transition frequency σ_0 , the strength S and the width α . The following discussion covers a technique used for extraction of these parameters when the data to be analyzed contain the line overlapping.

The first step in the analysis was to separate the data into groups of lines which were sufficiently isolated from others, and then the second step was to apply the curve fitting technique based on the least-square method. The first process was necessary because the data contained a variable degree of line overlapping. The groups were separated by a sufficient zero absorptance interval from their neighbors at their both sides. With the line center frequency determined as described above, the remaining two variables for each component line, the strength and the width, were determined under the assumption that the line profile was Lorentzian. A spectral pattern theoretically constructed using the Lorentzian profile with assumed parameters was compared with the observed data. The square error between them was calculated and then it was

minimized by adjusting the two variables, the strength and the width, for each component line. The sequence, which was the non-linear least-square-curve fitting process, was repeated to reduce the square error to a stationary value which was expected for a noise level of the observed data. After the error figure converged to a stationary value, the integrated absorptance W ,

$$W = \int A(\sigma) d\sigma, \quad (7)$$

was calculated for each line contained in the group using the strength and the width thus established. The standard method of obtaining the integrated absorptance by numerically integrating the observed absorptance for each line was not applicable to our data reduction, because the data contained a considerable overlapping of the lines.

The Lorentzian profile assumption used in our data analysis was in principle improper. The H_2O pressure was taken always very low in our data measurement for reduction of the line overlapping to a minimum level. The expected collision width was much smaller than the Doppler width under such a condition. We adopted the Lorentzian absorption because of the following reason. For weak lines a question of the line width did not matter because the integrated absorptance W and the strength held a linear relationship independent of the width. For strongly saturated lines, the observable absorptance contour was the wing section which was Lorentzian. The central peak region of such lines was completely saturated. The integrated absorptance W was controlled by the wing section and thus by the Lorentzian profile. The line profile in the center peak region produced a very small effect in determination of the integrated absorptance. Thus the Lorentzian profile assumption was a practical choice for extraction of the integrated absorptance even though it was theoretically improper. Once the integrated absorptance was determined, it was used to derive the

final strength value. For the Lorentzian line which was strongly saturated at the center, a strong interdependence existing between the strength S and the width α made their separate determination very impractical. With the integrated absorptance and the absorptance contour fixed, a quantity \sqrt{S} was the only meaningful parameter which could be determined for such a line, even when a noise level in the data was exceptionally small. We adopted the theoretically accepted value for α^2 in derivation of the strength S and the integrated absorptance. The width was extrapolated at 800°K from the values calculated for room temperature using a simple impact theory assumption:

$$\alpha(T) = \alpha(295) \left(\frac{295}{T} \right)^{1/2}.$$

Results and Discussion

The results obtained in the present study are summarized in Table I. The data listed in the table are the line frequency in cm^{-1} , the strength S in $(\text{cm}^{-1}/\text{molecule cm}^{-2})$ at 800°K, the observed integrated absorptance for an observation condition $\nu_{\text{obs}} = 1.1 \times 10^4 \text{ cm}$, $T = 800^\circ\text{K}$ and $\ell = 150 \text{ cm}$, the lower state energy in cm^{-1} , the termite identification (A'' , K'' , K''''), (C'' , K'' , K''''), (A'' , C'' , K''), (A'' , C'' , K''''), the termite identification code, the intensity ratio, the line width expressed as the difference between the observed transition frequency and the value listed in the latest AFGL line listing. The data are arranged in increasing order of the observed line position. Figure 1 shows four spectral data, the raw spectrum observed at the H_2O column density of 1.17×10^{19} molecules over 350 cm absorption path at 800°K, the absorptance spectrum derived for the analysis, the synthetic spectrum calculated using the parameters determined in the analysis, and the spectrum synthesized using the parameters given in the latest AFGL line listing. The data listed in Table I contain those lines

newly identified in the present study, which are the high J lines of the $(v_2=0)$ and the $(2v_2-v_2)$ transitions. We were able to follow the v_2 transitions up to the $(2^4_{1,24}-2^4_{0,23})-(2^4_{0,24}-2^4_{1,23})$ doublet, and the $(2v_2-v_2)$ transition up to the $(20_{1,20}-19_{0,19})-(20_{0,20}-19_{1,19})$ doublet. The highest excitation energy observed at 800°K in our data exceeded 5000 cm^{-1} .

Table II summarizes those lines which were either newly assigned or quite different from the latest AFGL line listing.

One thing noticed as peculiar in the present study was that the strongly saturated lines had a central peak much narrower than that theoretically constructed. The pronounced wing absorption was found to produce no matching to a sharp central peak. The synthetic spectrum shown in the third row of Figure 1 was generated by the Lorentzian line profile which had the narrowest central peak of the other profiles, the Gaussian and the Voigt. For an example, the doublet $(11_{0,11}-10_{1,10})$ and $(11_{1,11}-10_{0,10})$ of the v_2 band exhibited two sharp peaks, one at 1801.3260 and another at 1801.3621, clearly separated in the observed data. The synthetic spectrum, the third trace of Figure 1, failed to show a corresponding central structure. The observed data indicated that the central region was far narrower than the peak structure which could have been theoretically constructed for the observed wing region. No explanations were found to this observation.

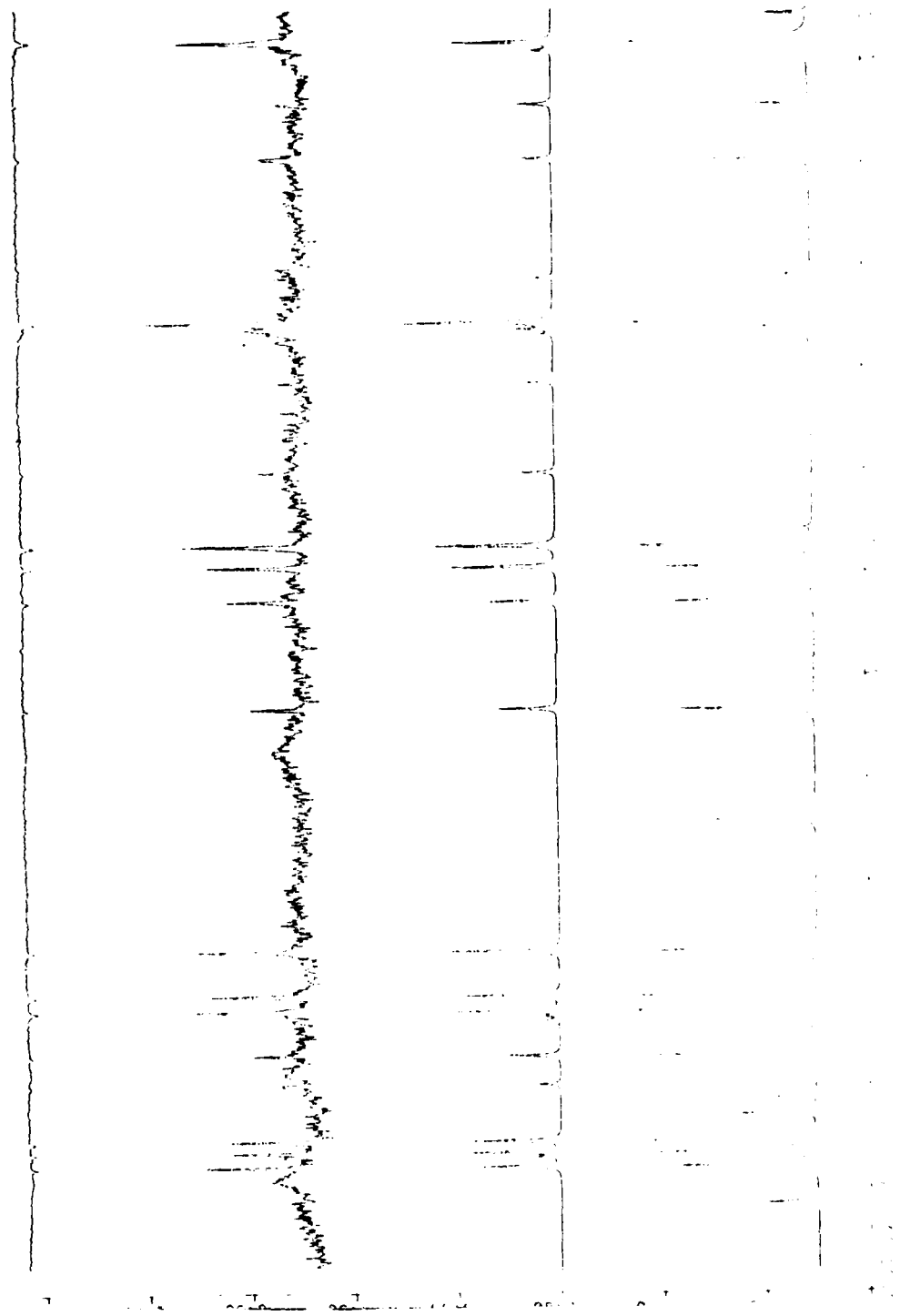
References

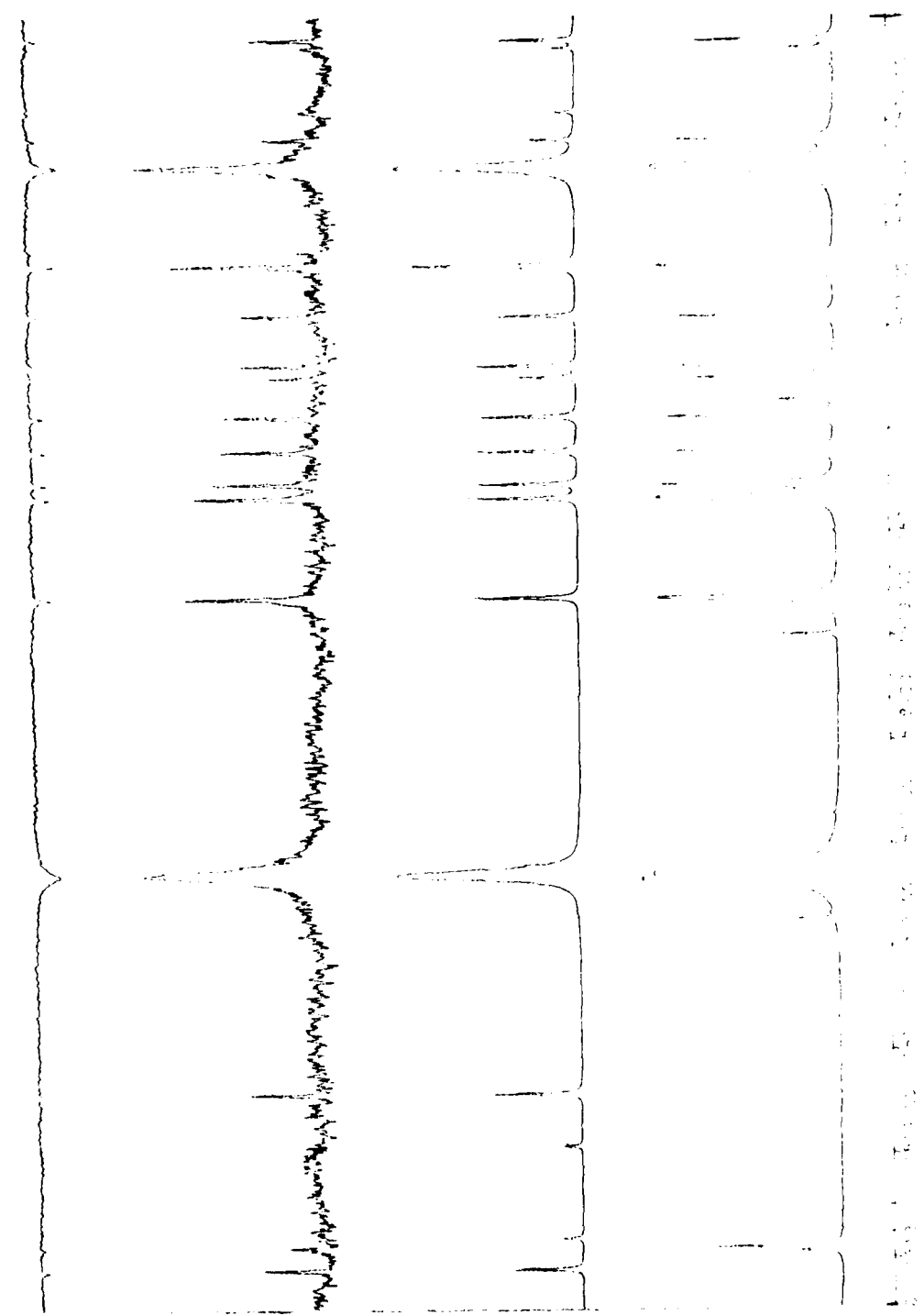
1. R.A. McClatchey *et al*, AFCRL Report No. 434, TR-73-0096 (1973).
The line compilation data is available to the public in the form of a magnetic tape. It is obtained from the National Climatic Center of NOAA, Environmental Data Service, Federal Building, Asheville NC 28801. The data have been updated several times since 1973 for accommodating improvements.
2. J.M. Flaud and C. Camy-Peyrot, J. Mol. Spec. 51, 142 (1974).
J.M. Flaud *et al*, Mol. Phys. 32, 499 (1976).
C. Camy-Peyrot *et al*, Mol. Phys. 33, 1641 (1977).
3. J.H. Taylor, W.S. Benedict and J. Strong, J. Chem. Phys. 12, 1884 (1954).
Y. Ben Aryeh, J.Q.S.R.T. 7, 201 (1967).
Shau-Yau Ho, Infrared Physics 14, 37 (1974).
4. H. Sakai, "High-Resolving Power Fourier Spectroscopy" in Spectrometric Techniques, Vol. I, G. Vanasse, Ed., Academic Press, New York (1977).
5. K.D. Mielenz *et al*, Appl. Phys. Letters 7, 277 (1965).
6. J. Terrien, J. Phys. Rad. 19, 390 (1958).
7. G. Guelachvili, "These," Université de Paris-Sud (1973).
8. W. Dalton and H. Sakai, Appl. Opt. 19, 2413 (1980).
9. W.S. Benedict and L. Kaplan, J.Q.S.R.T. 4, 453 (1964).
W.S. Benedict and L. Kaplan, J. Chem. Phys. 30, 388 (1959).

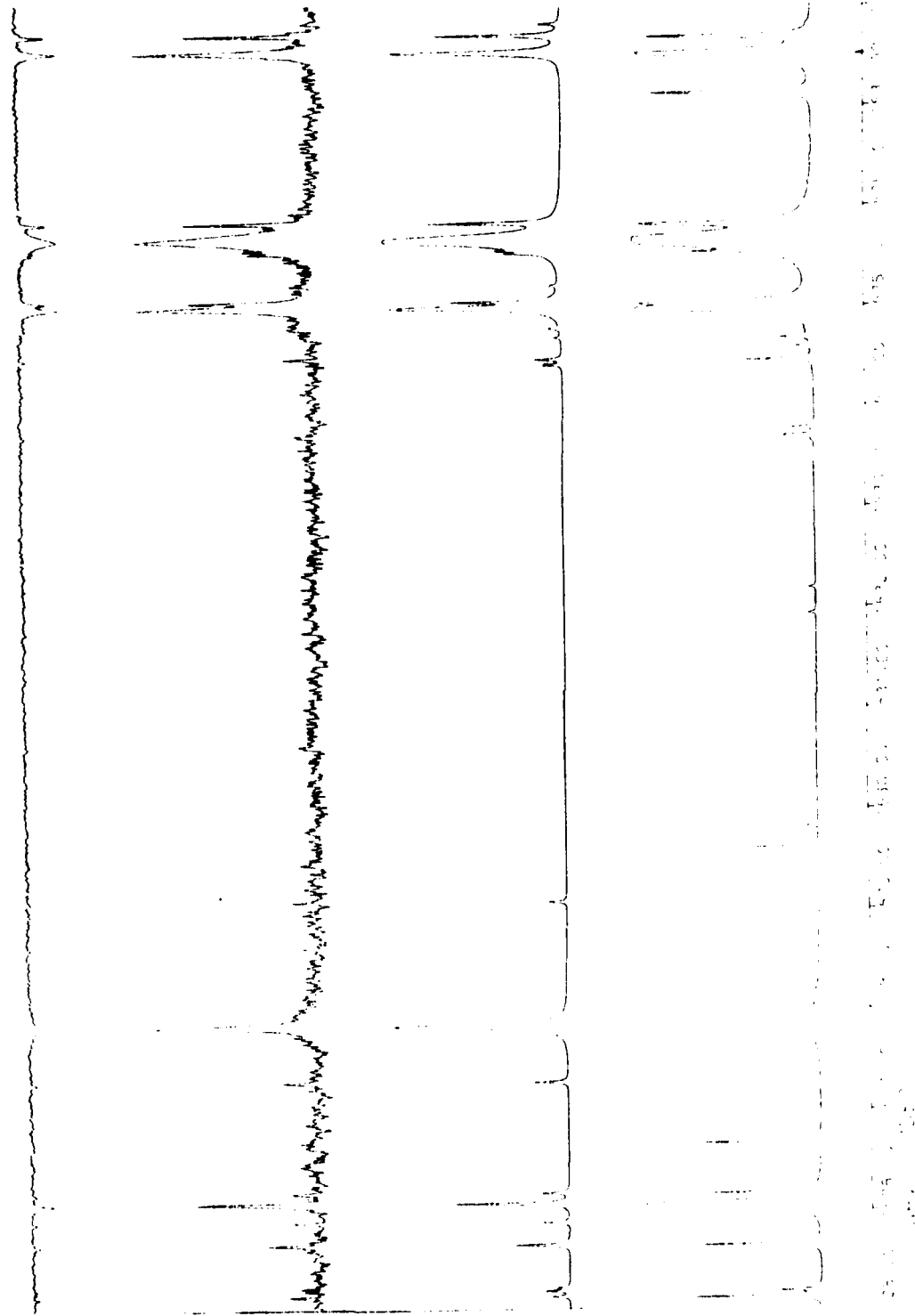
Figure 1

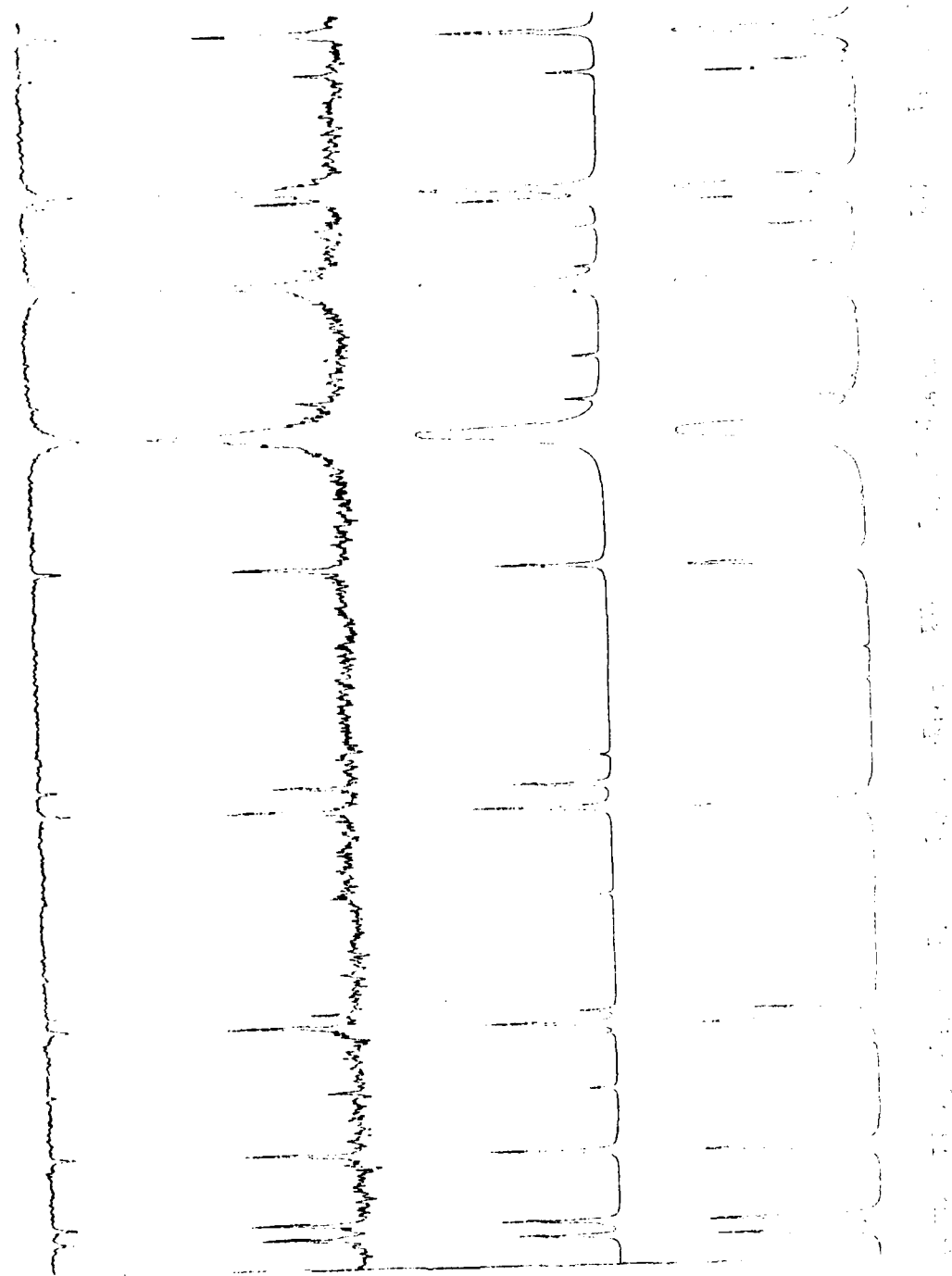
Atlas of H_2O absorption spectrum between $1600 \sim 2000 \text{ cm}^{-1}$ taken at the gas temperature = 800°K , the absorption path = 350 cm , the H_2O pressure = 6.0 torr (no other gases added), and the spectral resolution = 0.0060 cm^{-1} . The top trace is the raw data. The second is the absorptance data determined from the raw data. The third is the absorptance spectrum synthesized from the line parameters determined in the present work. The bottom trace is the absorptance spectrum synthesized for the same condition using the line parameters of the current AFGL listing (1980 version).

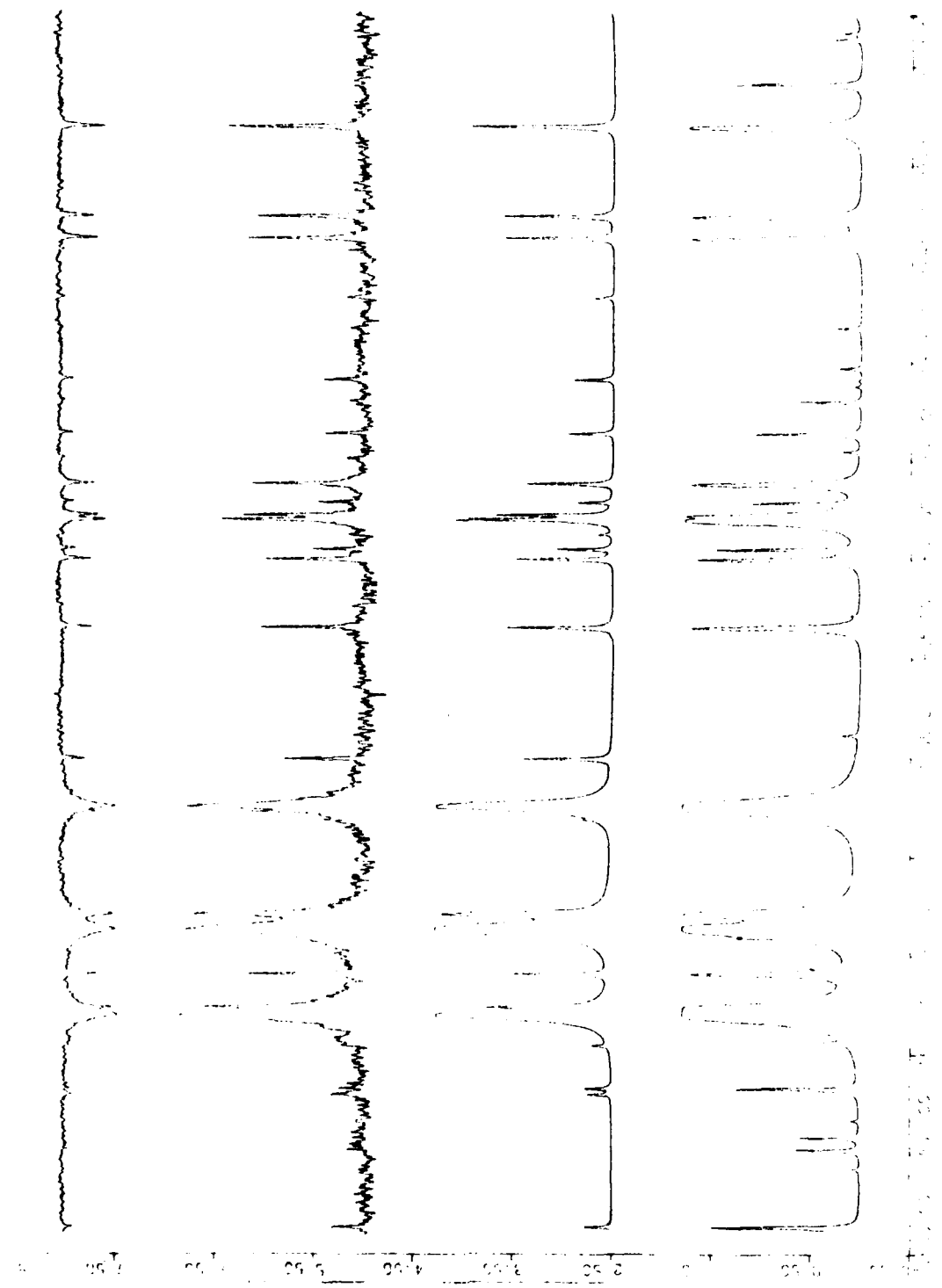
Figure 1

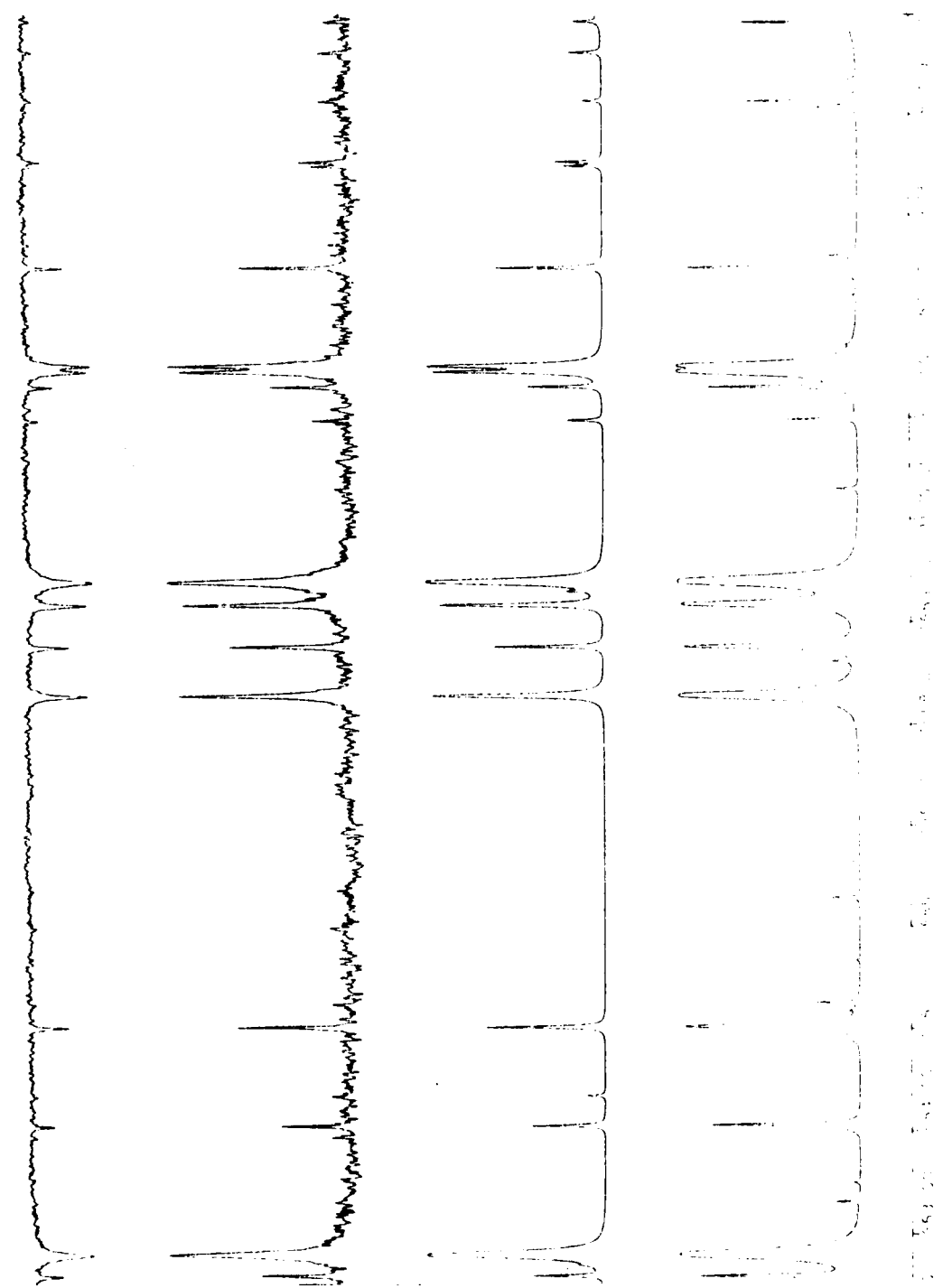


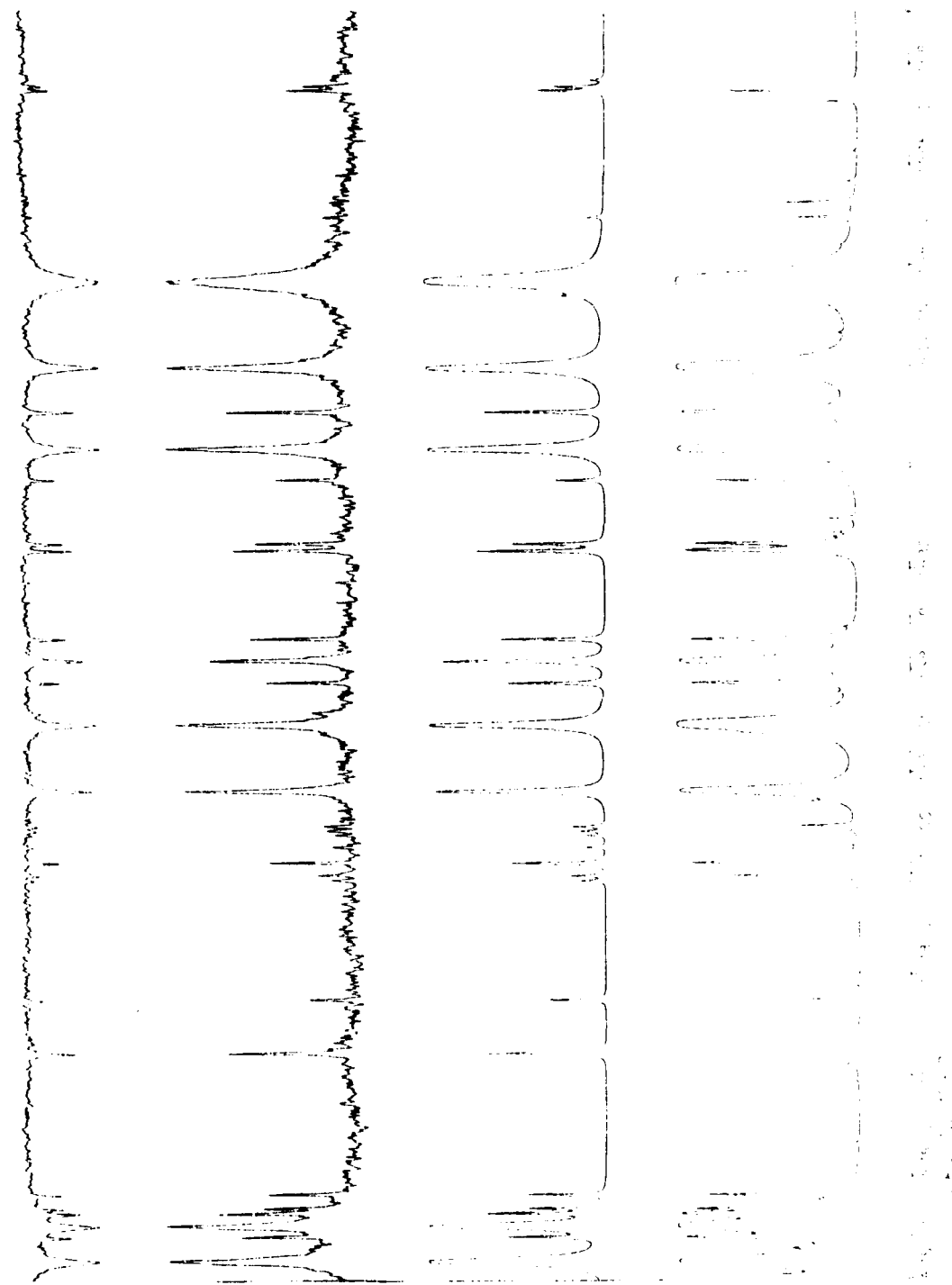


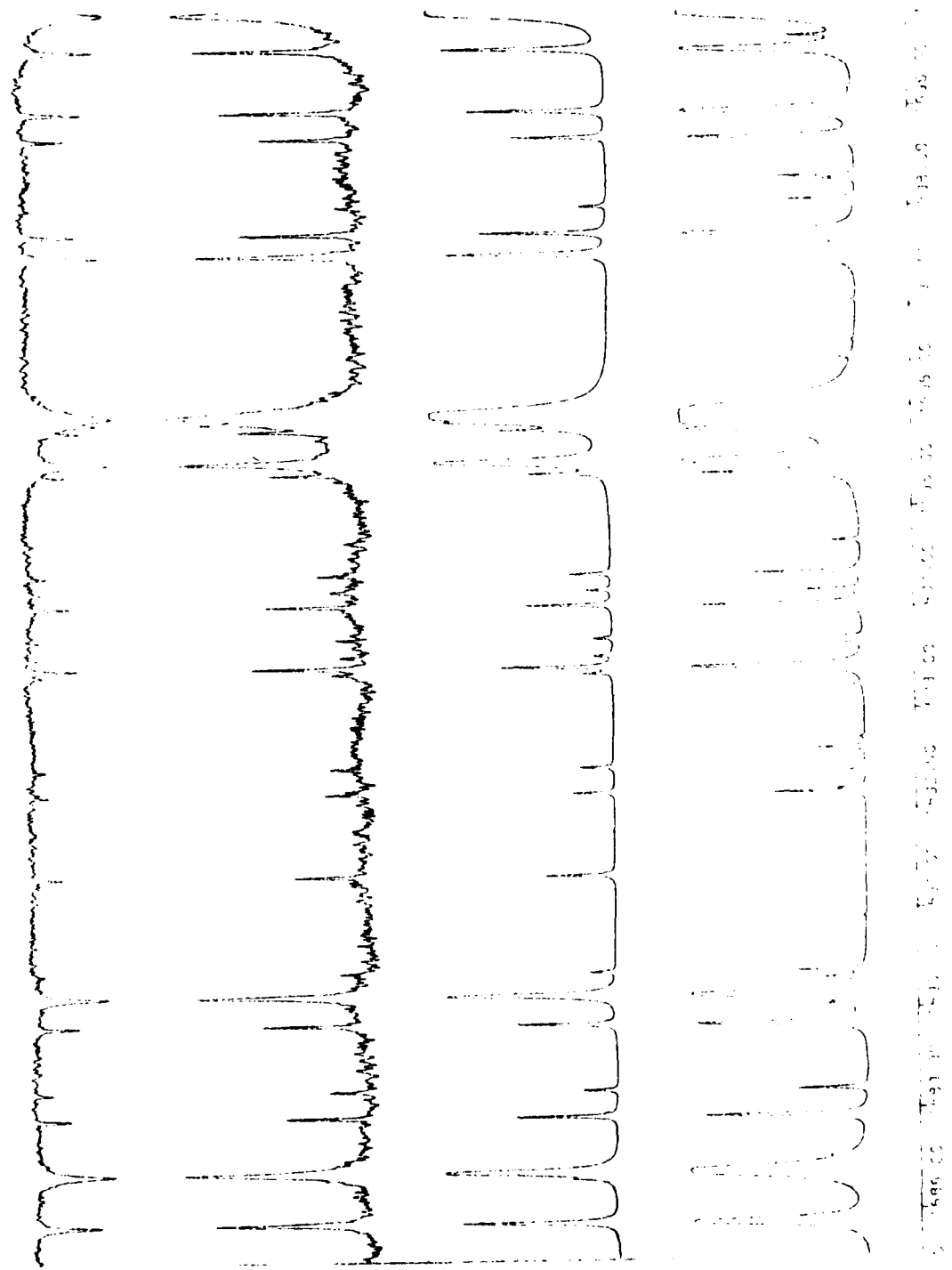


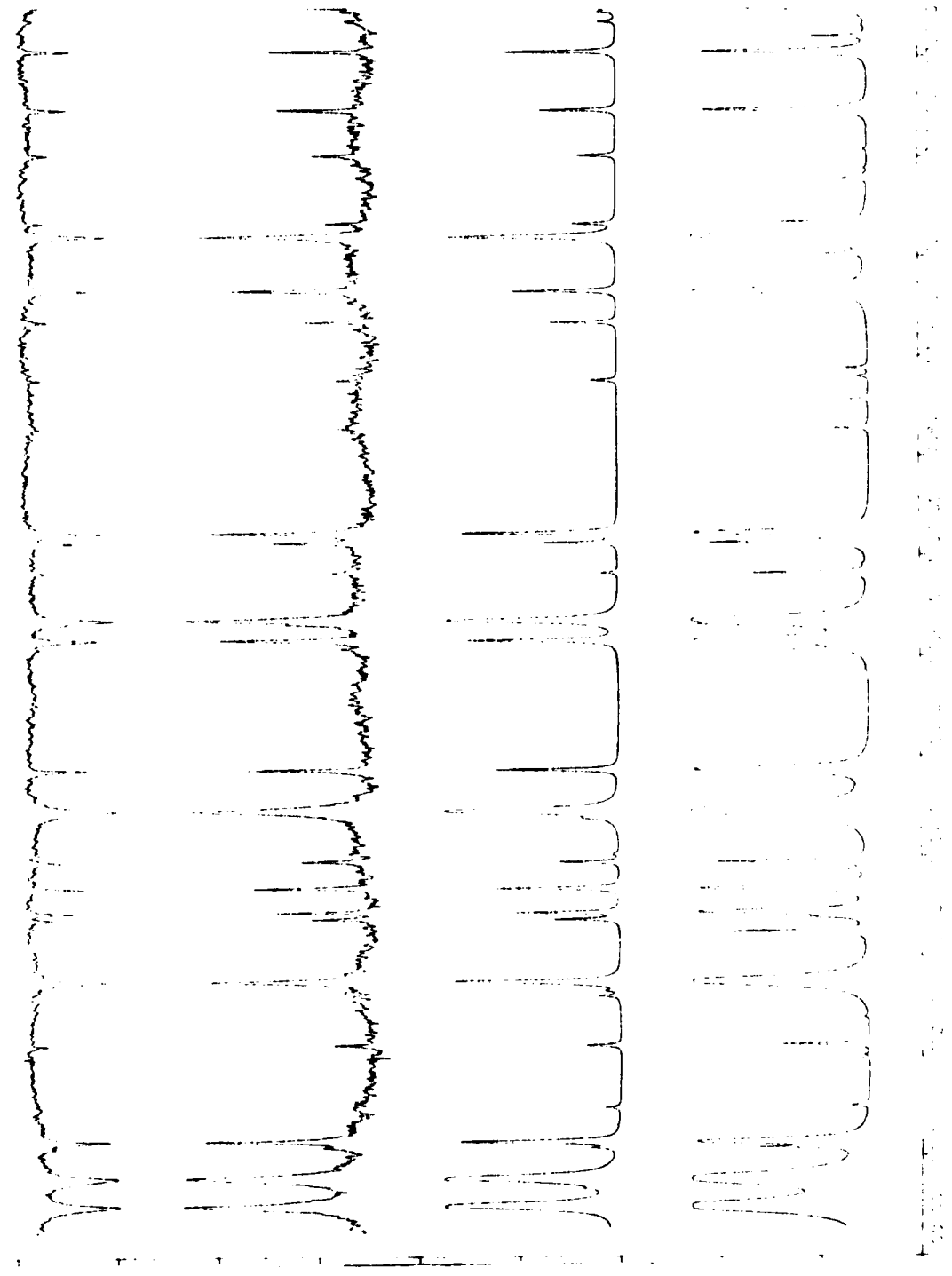


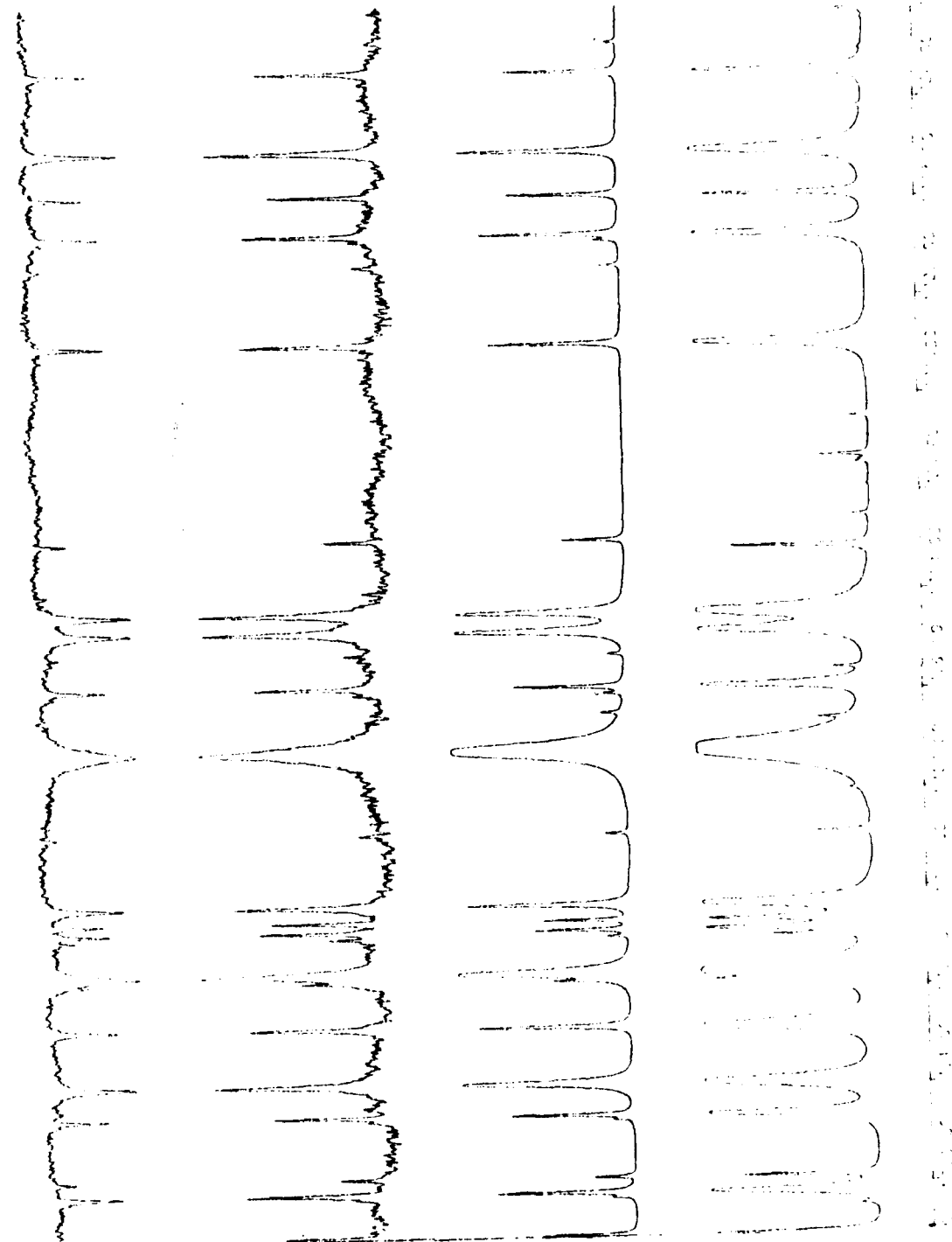




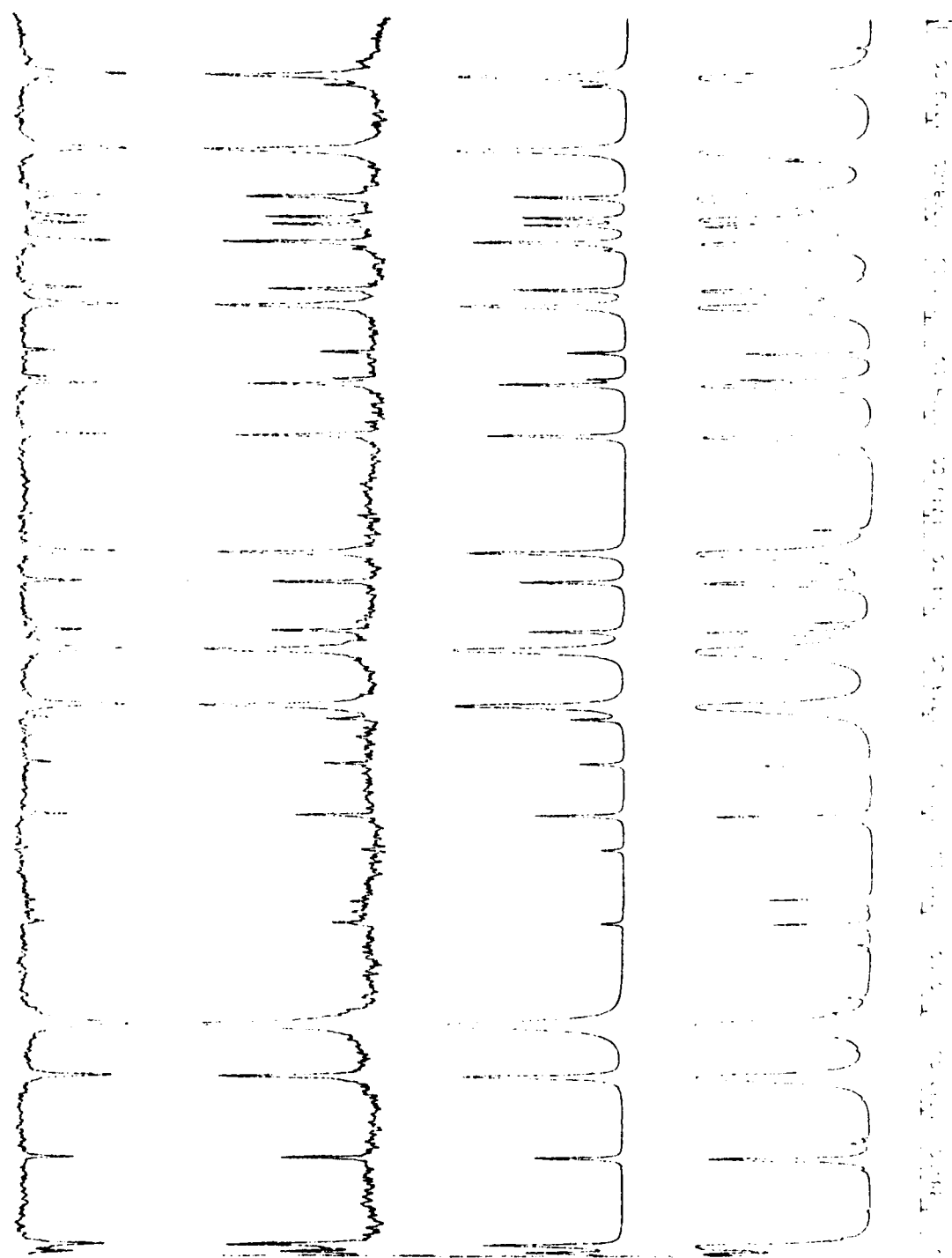


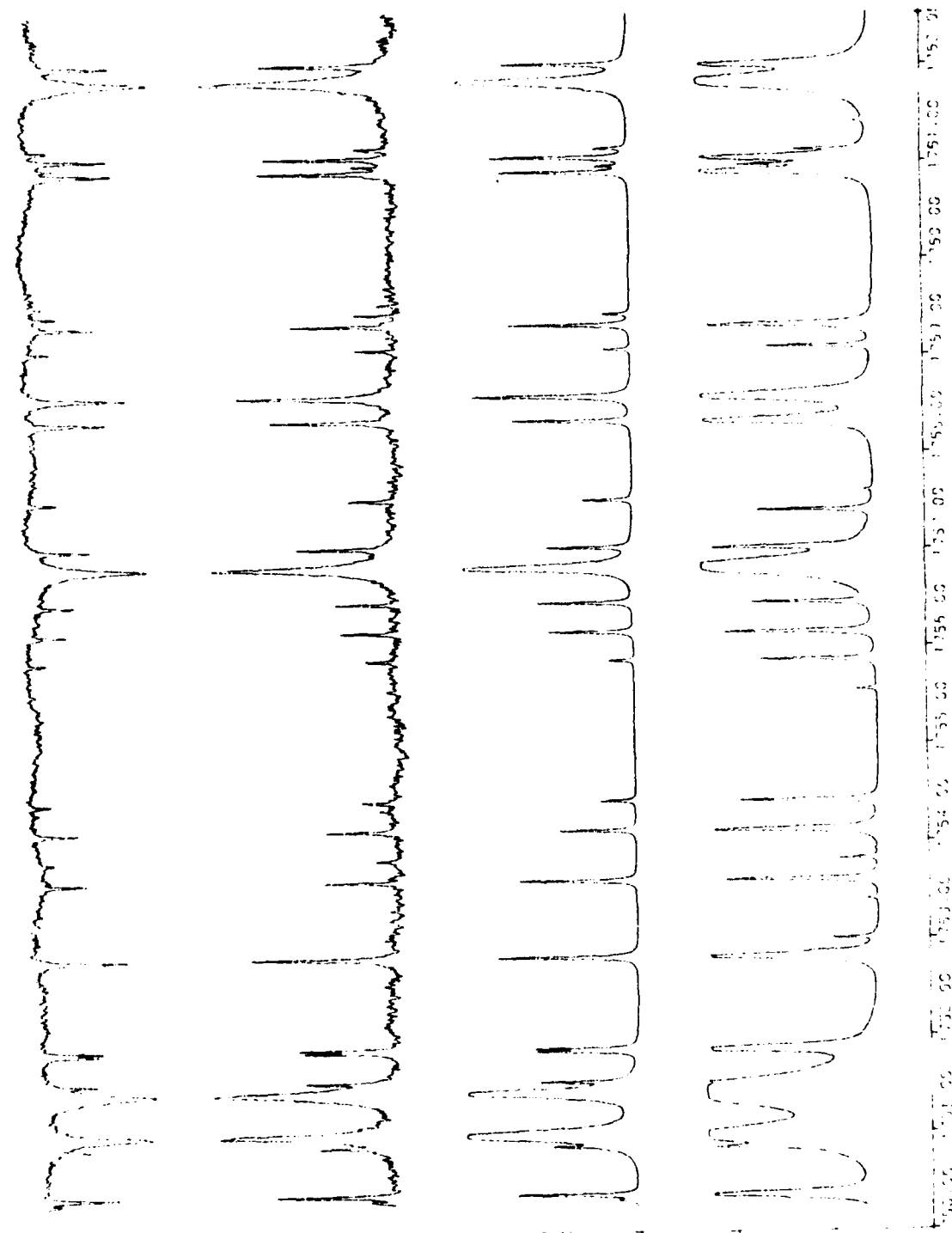


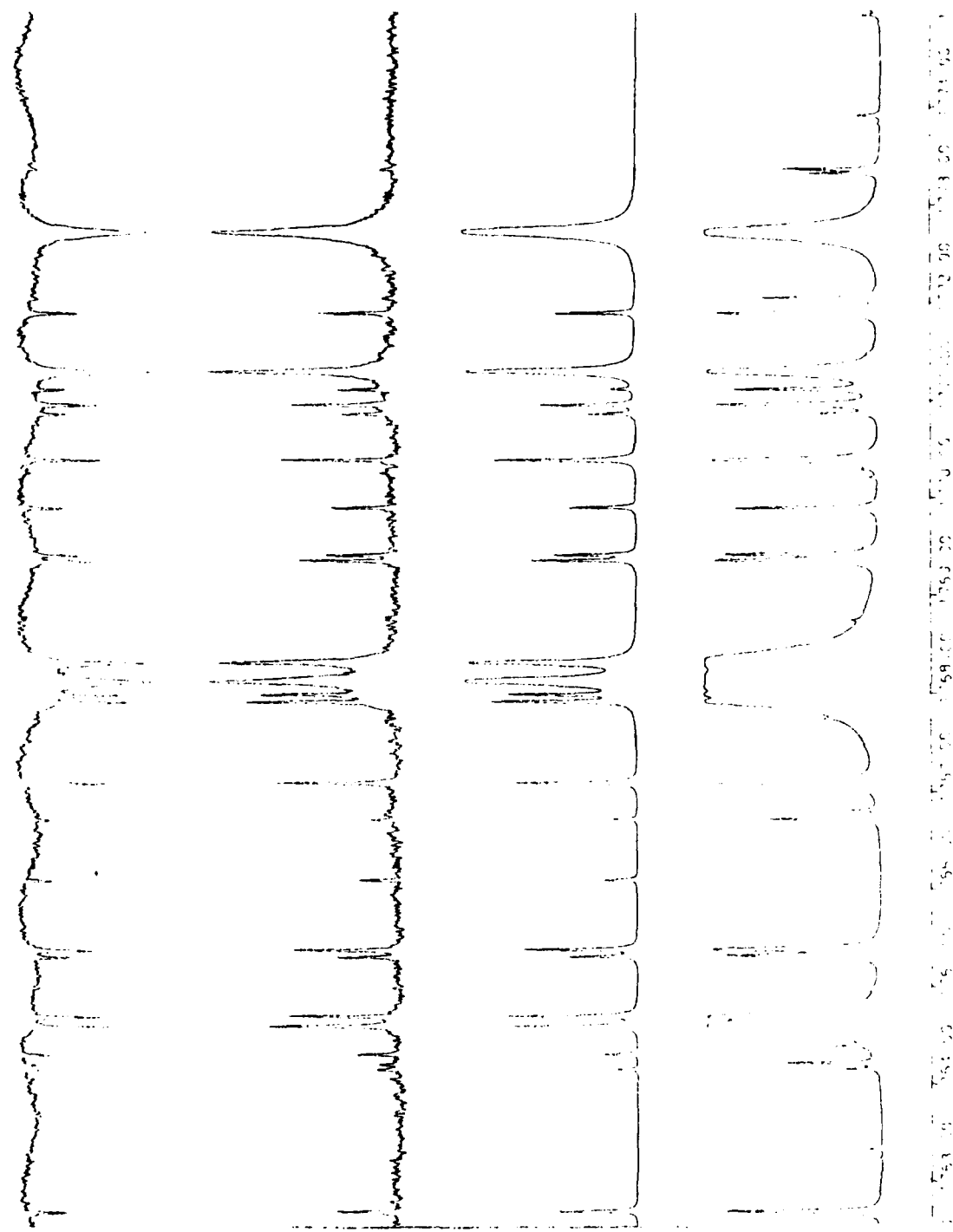


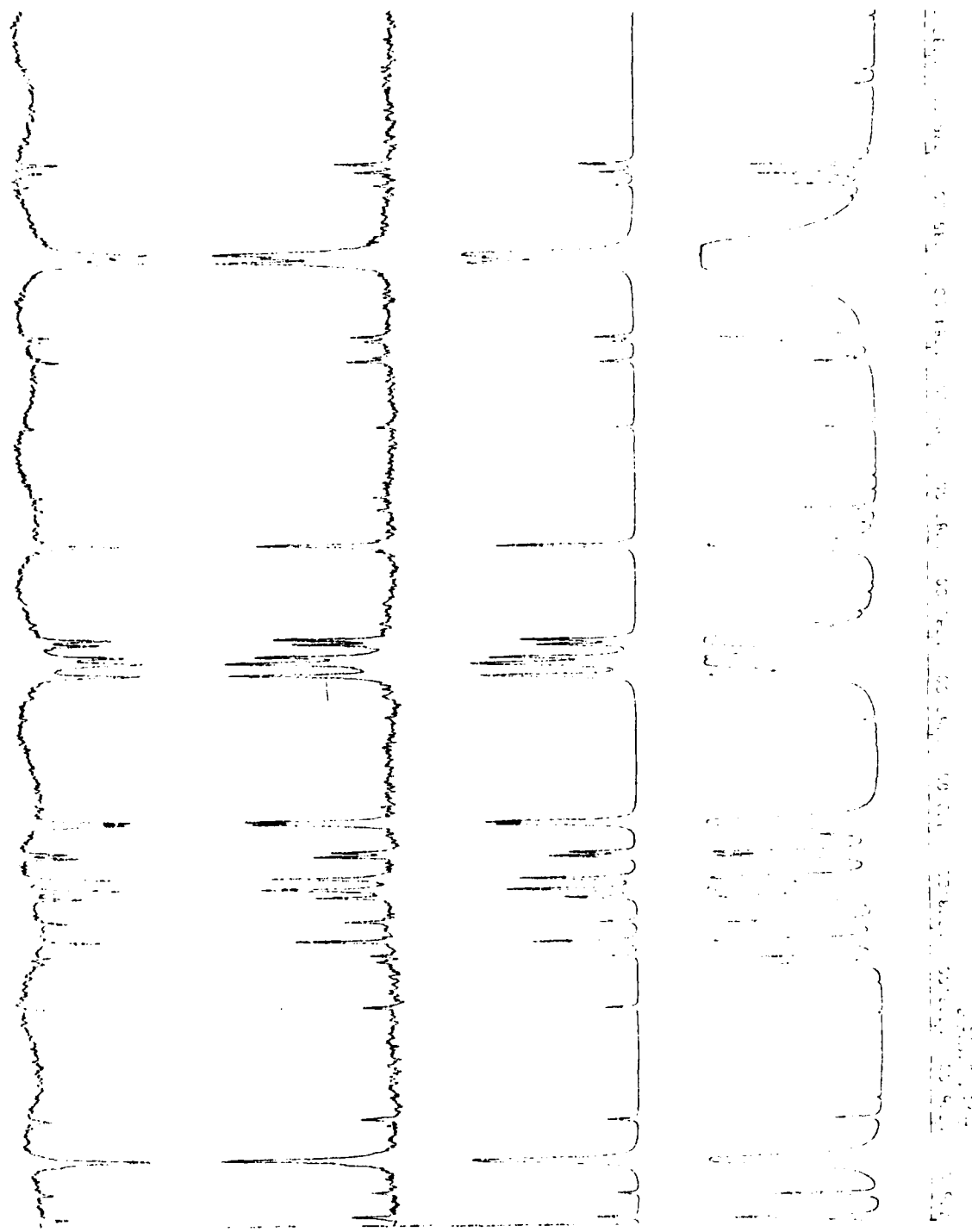


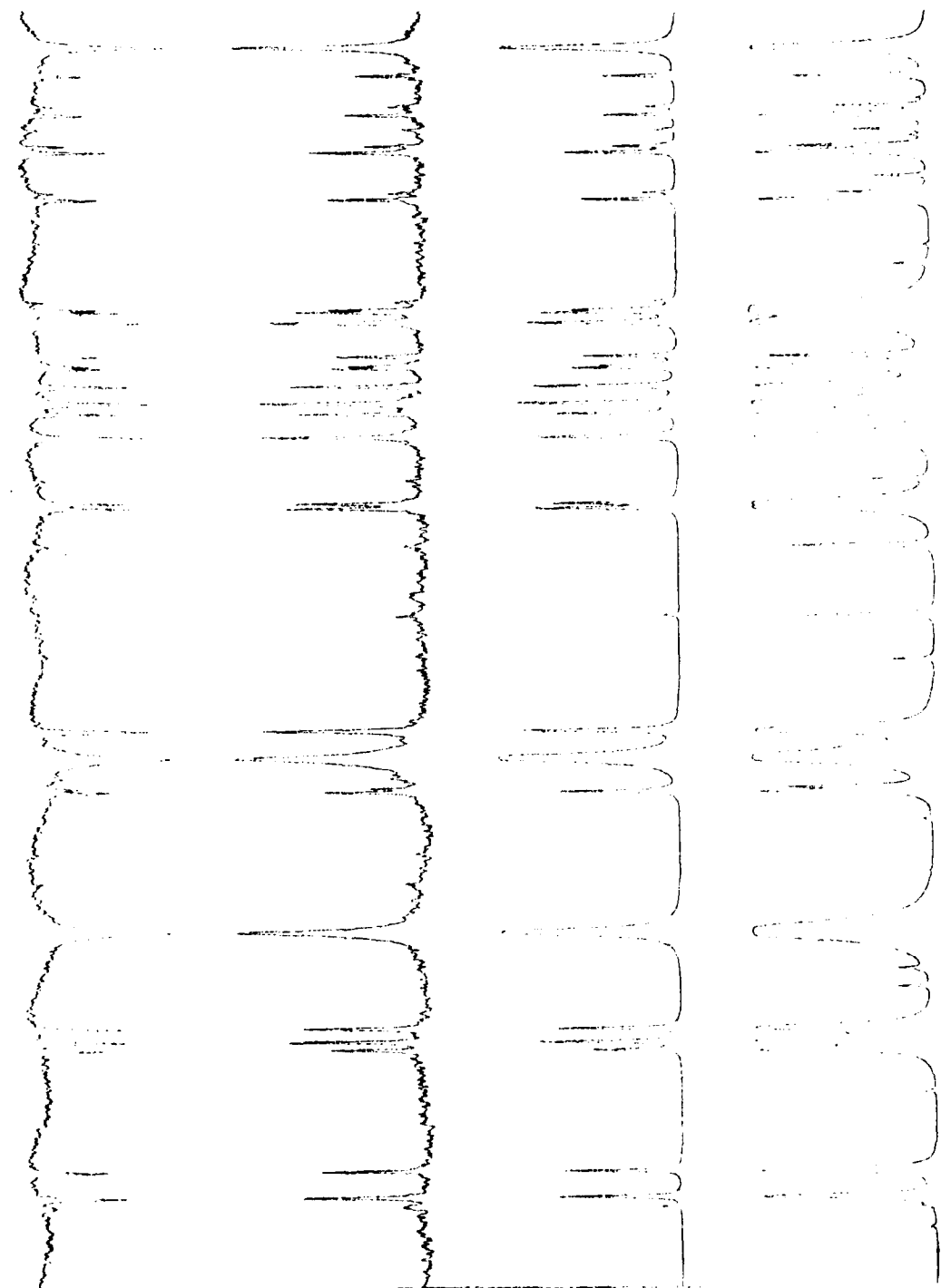


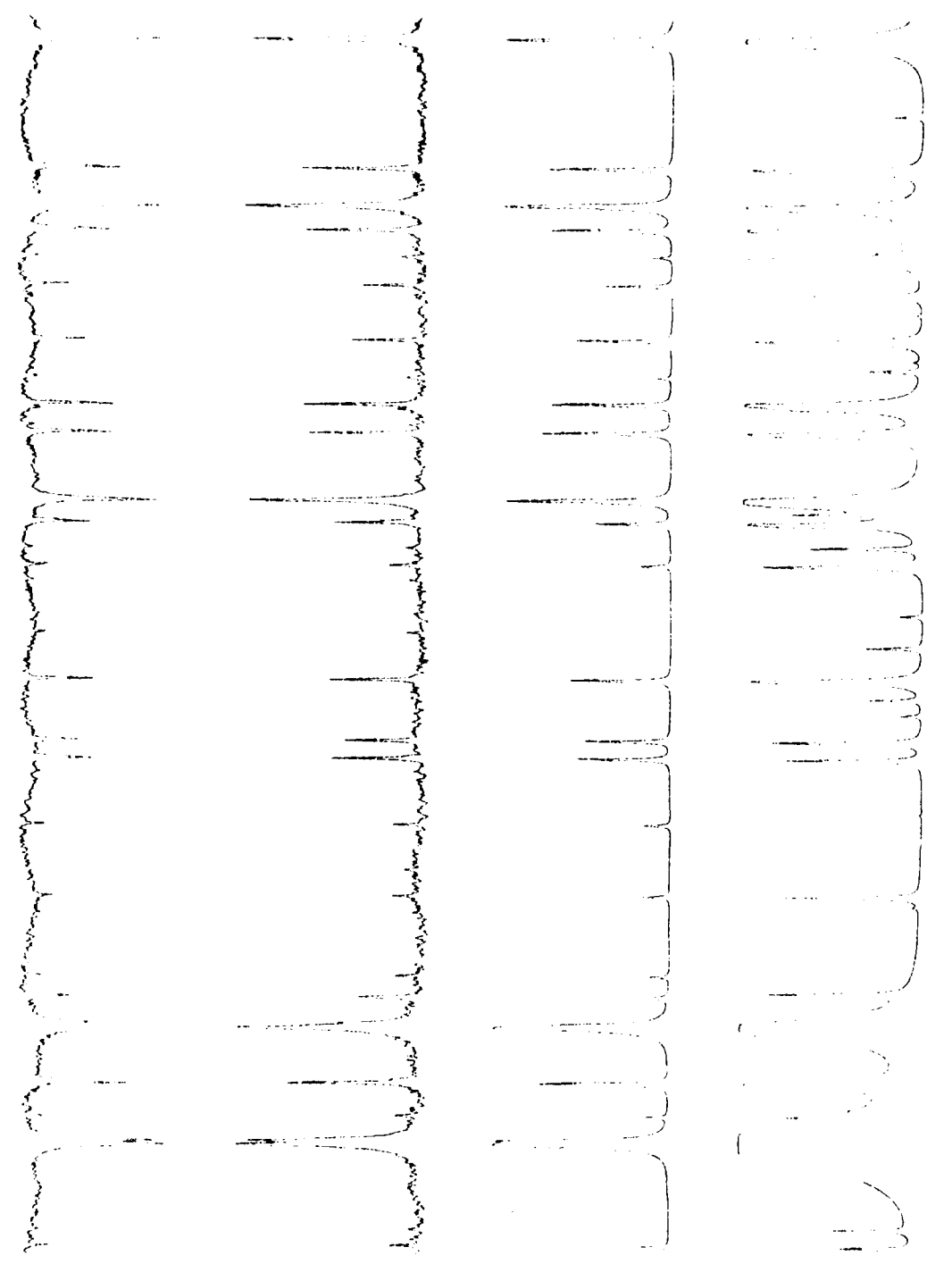


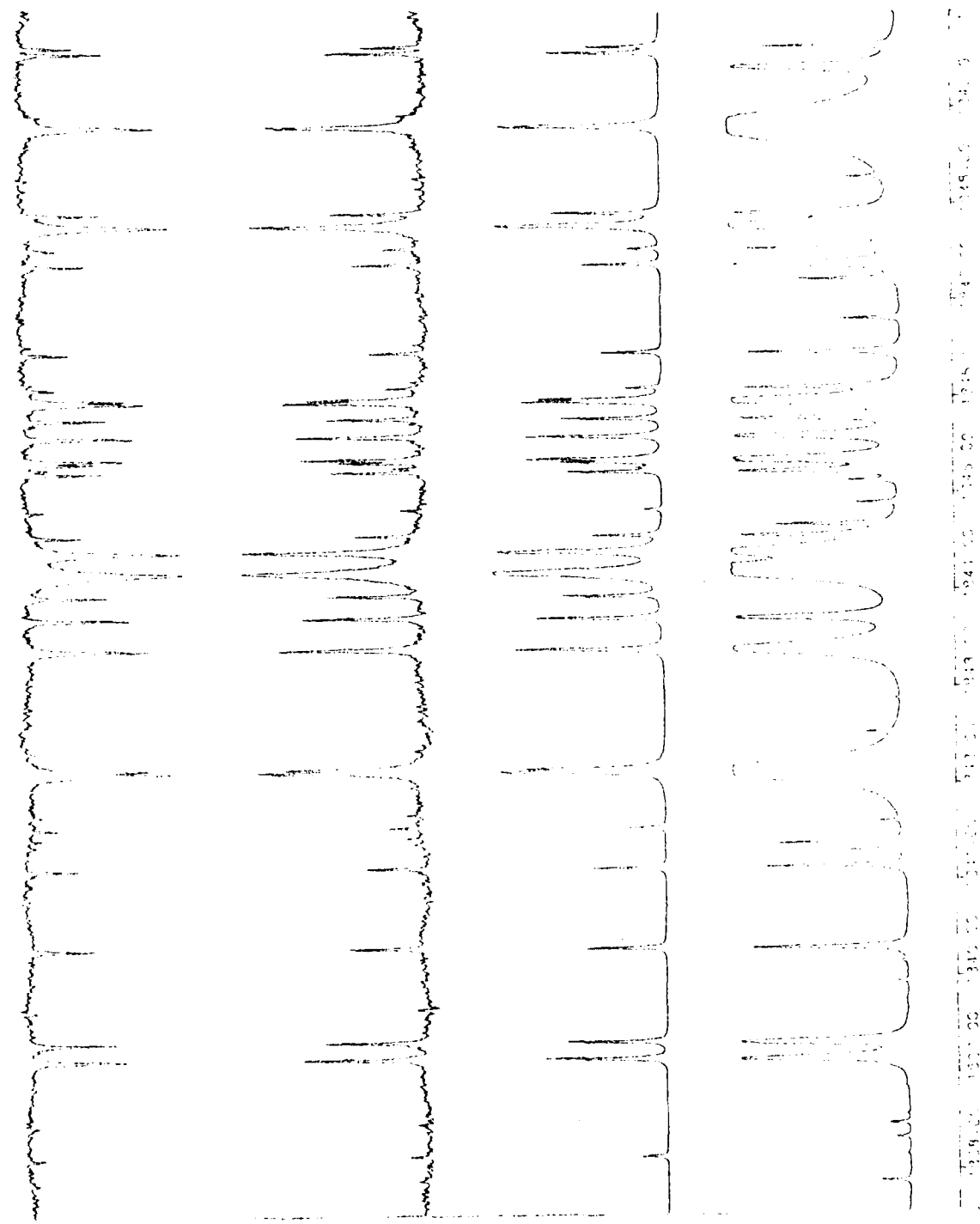


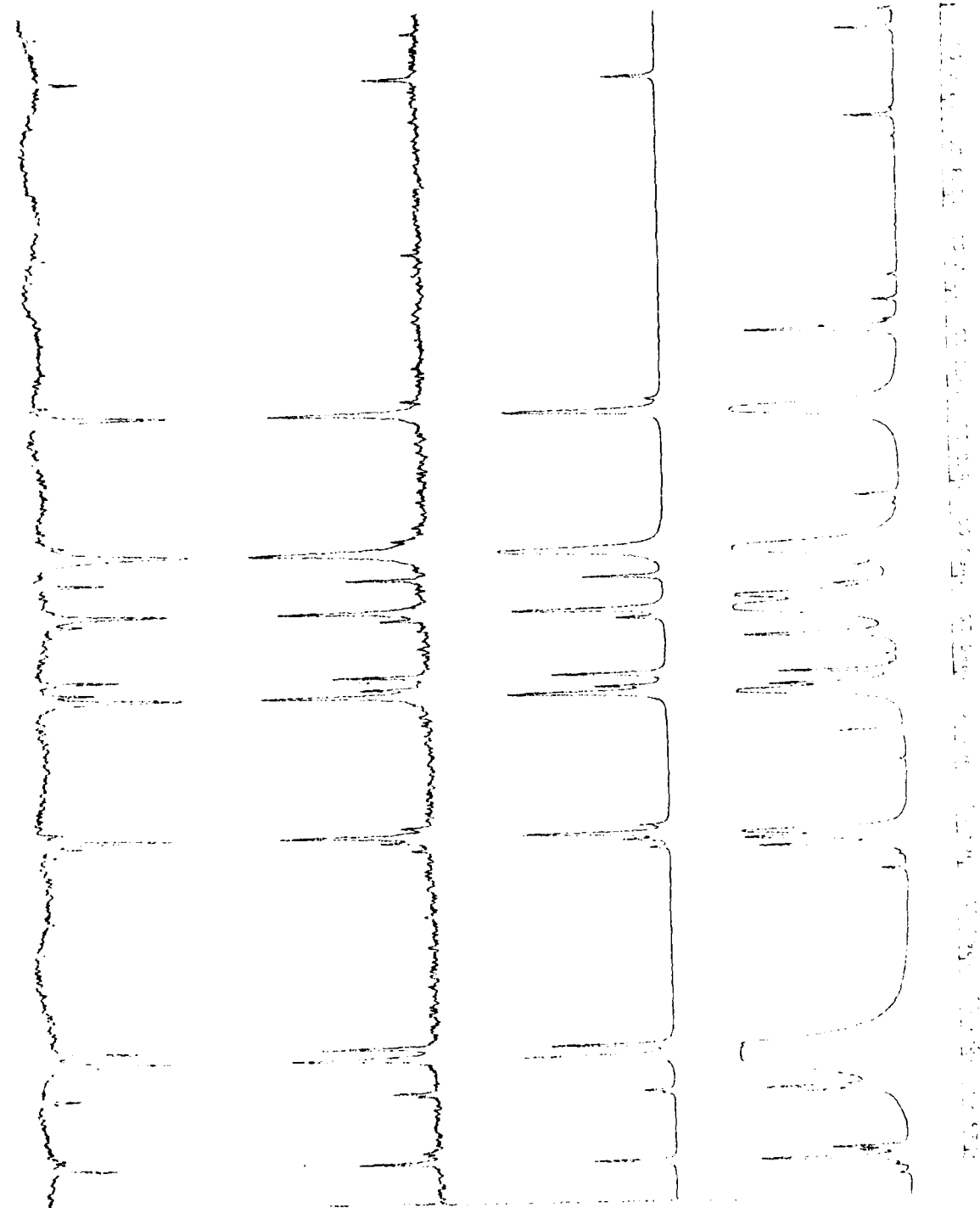






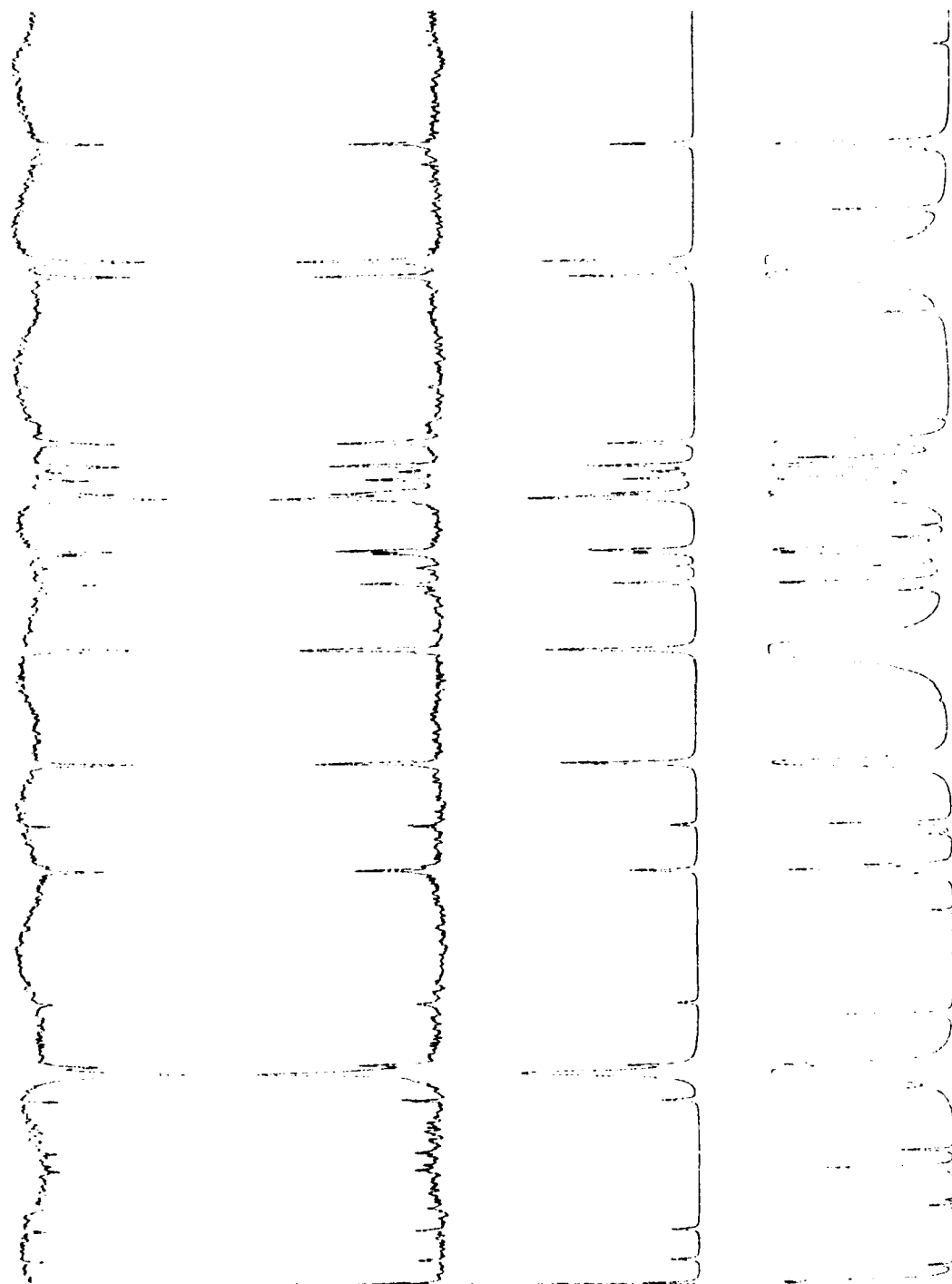






1. *Leucostethus* *leucostethus* *leucostethus*

2. *Leucostethus* *leucostethus* *leucostethus*



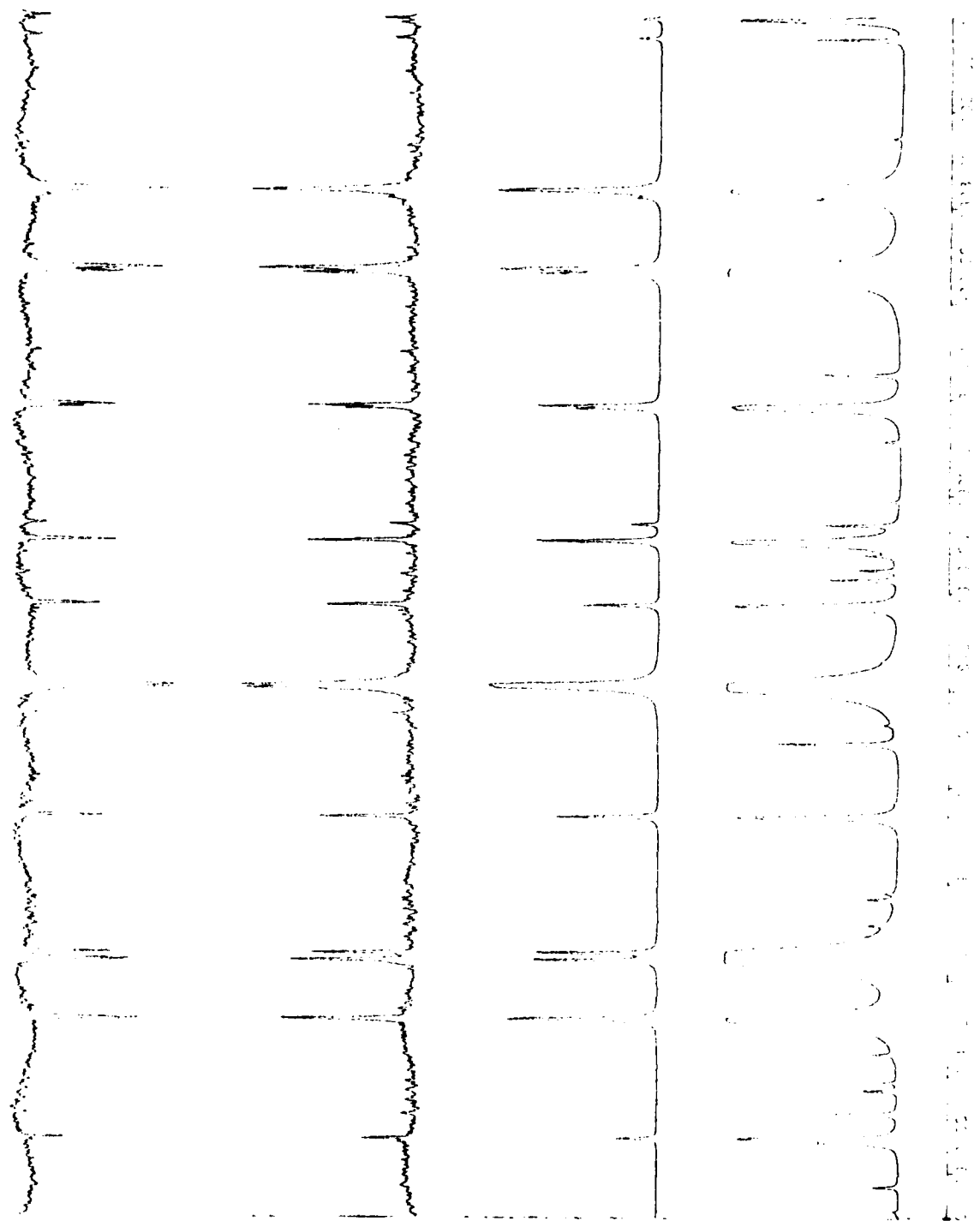
卷之三

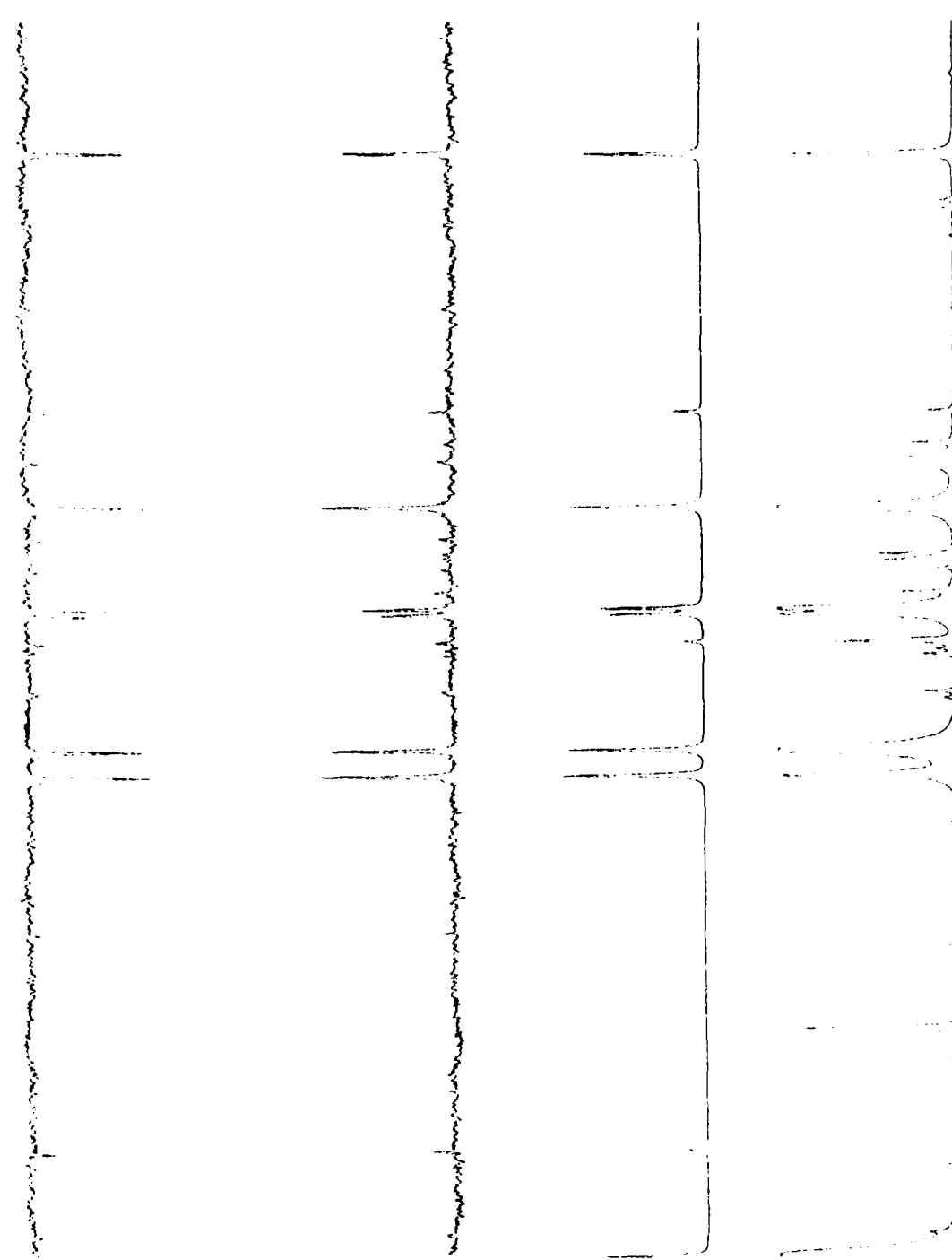
وَلَمْ يَرْجِعْ إِلَيْهِ أَنْفُسُهُمْ إِنْ هُمْ بِذَكْرِهِ إِذَا مَا يَرَوْنَ

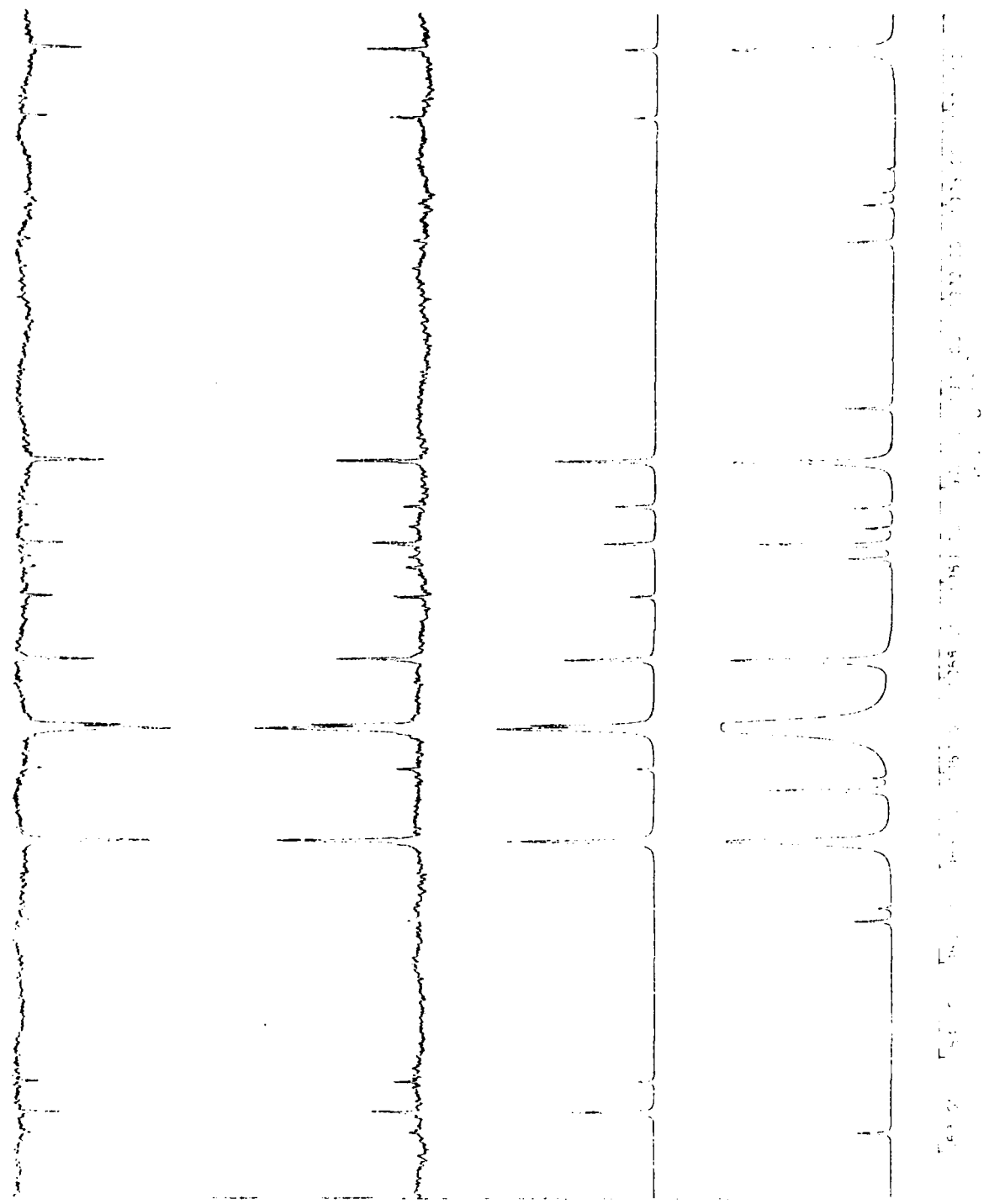
卷之三

1. *Leucosia* *leucosia* (L.) *leucosia* (L.)

卷之三







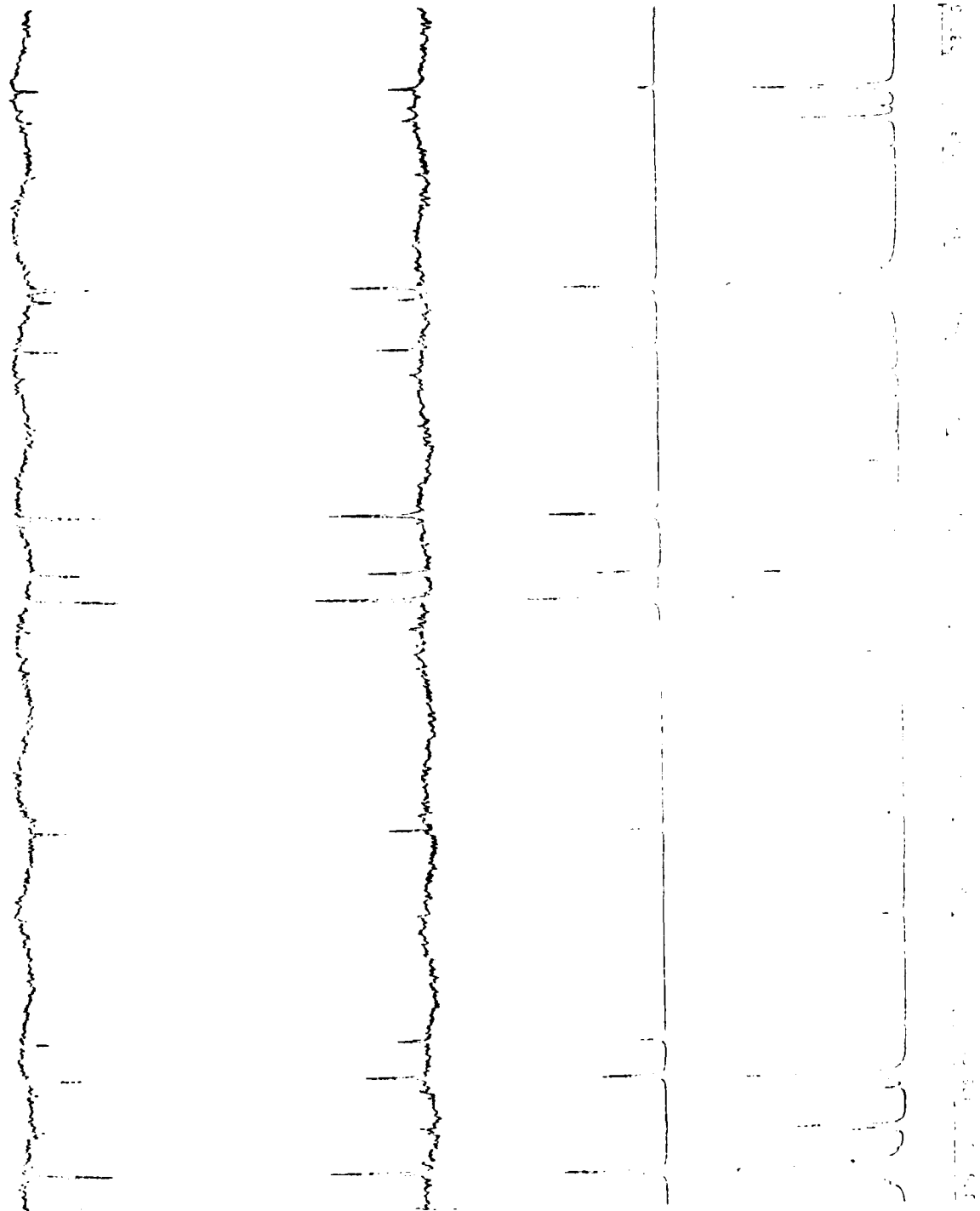


Table I

H_2O line data between 1600 cm^{-1} and 2000 cm^{-1} .

The listings are:

- the transition frequency in cm^{-1}
- the absorption strength in $\text{cm}^{-1}/\text{molecule cm}^{-2}$ at 800°K
- the integrated absorptance in cm^{-1} for the H_2O column density 2.17×10^{20} molecules/ cm^2 at 800°K
- the lower state energy in cm^{-1}
- the transition assignment in (J', KA', KC') , (J'', KA'', KC'') , (v_1', v_2', v_3') , and (v_1'', v_2'', v_3'')
- the internal code
- the isotope code
- the molecule identification code
- the integrated absorptance, and
- the wavenumber difference between the measured and the one listed in the AFGL listing.

Table I

1	2	3	4	5	6	7	8	9	10	11	12	13	14	15	16	17	18	19	20	21	22	23	24	25	26	27	28	29	30	31	32	33	34	35	36	37	38	39	40	41	42	43	44	45	46	47	48	49	50	51	52	53	54	55	56	57	58	59	60	61	62	63	64	65	66	67	68	69	70	71	72	73	74	75	76	77	78	79	80	81	82	83	84	85	86	87	88	89	90	91	92	93	94	95	96	97	98	99	100
1	2	3	4	5	6	7	8	9	10	11	12	13	14	15	16	17	18	19	20	21	22	23	24	25	26	27	28	29	30	31	32	33	34	35	36	37	38	39	40	41	42	43	44	45	46	47	48	49	50	51	52	53	54	55	56	57	58	59	60	61	62	63	64	65	66	67	68	69	70	71	72	73	74	75	76	77	78	79	80	81	82	83	84	85	86	87	88	89	90	91	92	93	94	95	96	97	98	99	100

.....

1	2	3	4	5	6	7	8	9	10	11	12	13	14	15	16	17	18	19	20	21	22	23	24	25	26	27	28	29	30	31	32	33	34	35	36	37	38	39	40	41	42	43	44	45	46	47	48	49	50	51	52	53	54	55	56	57	58	59	60	61	62	63	64	65	66	67	68	69	70	71	72	73	74	75	76	77	78	79	80	81	82	83	84	85	86	87	88	89	90	91	92	93	94	95	96	97	98	99	100
1	2	3	4	5	6	7	8	9	10	11	12	13	14	15	16	17	18	19	20	21	22	23	24	25	26	27	28	29	30	31	32	33	34	35	36	37	38	39	40	41	42	43	44	45	46	47	48	49	50	51	52	53	54	55	56	57	58	59	60	61	62	63	64	65	66	67	68	69	70	71	72	73	74	75	76	77	78	79	80	81	82	83	84	85	86	87	88	89	90	91	92	93	94	95	96	97	98	99	100

१०८ अनुवाद द्वारा अनुवाद करने वाले विद्युत विभाग द्वारा दिए गए अनुवाद के अनुसार इस अधिकारी का नाम है।

PERIODIC TESTS OF THE HUMORAL IMMUNE RESPONSE ARE USEFUL FOR MONITORING THE PROGRESS OF DISEASE.

211-212 213-214 215-216 217-218 219-220 221-222 223-224 225-226 227-228 229-230 231-232 233-234 235-236 237-238 239-240 241-242 243-244 245-246 247-248 249-250 251-252 253-254 255-256 257-258 259-260 261-262 263-264 265-266 267-268 269-270 271-272 273-274 275-276 277-278 279-280 281-282 283-284 285-286 287-288 289-290 291-292 293-294 295-296 297-298 299-300 301-302 303-304 305-306 307-308 309-310 311-312 313-314 315-316 317-318 319-320 321-322 323-324 325-326 327-328 329-330 331-332 333-334 335-336 337-338 339-340 341-342 343-344 345-346 347-348 349-350 351-352 353-354 355-356 357-358 359-360 361-362 363-364 365-366 367-368 369-370 371-372 373-374 375-376 377-378 379-380 381-382 383-384 385-386 387-388 389-390 391-392 393-394 395-396 397-398 399-400 401-402 403-404 405-406 407-408 409-410 411-412 413-414 415-416 417-418 419-420 421-422 423-424 425-426 427-428 429-430 431-432 433-434 435-436 437-438 439-440 441-442 443-444 445-446 447-448 449-450 451-452 453-454 455-456 457-458 459-460 461-462 463-464 465-466 467-468 469-470 471-472 473-474 475-476 477-478 479-479 481-482 483-484 485-486 487-488 489-490 491-492 493-494 495-496 497-498 499-500 501-502 503-504 505-506 507-508 509-510 511-512 513-514 515-516 517-518 519-520 521-522 523-524 525-526 527-528 529-530 531-532 533-534 535-536 537-538 539-540 541-542 543-544 545-546 547-548 549-550 551-552 553-554 555-556 557-558 559-560 561-562 563-564 565-566 567-568 569-569 571-572 573-574 575-576 577-578 579-579 581-582 583-584 585-586 587-588 589-589 591-592 593-594 595-596 597-598 599-599 601-602 603-604 605-606 607-608 609-609 611-612 613-614 615-616 617-618 619-619 621-622 623-624 625-626 627-628 629-629 631-632 633-634 635-636 637-638 639-639 641-642 643-644 645-646 647-648 649-649 651-652 653-654 655-656 657-658 659-659 661-662 663-664 665-666 667-668 669-669 671-672 673-674 675-676 677-678 679-679 681-682 683-684 685-686 687-688 689-689 691-692 693-694 695-696 697-698 699-699 701-702 703-704 705-706 707-708 709-709 711-712 713-714 715-716 717-718 719-719 721-722 723-724 725-726 727-728 729-729 731-732 733-734 735-736 737-738 739-739 741-742 743-744 745-746 747-748 749-749 751-752 753-754 755-756 757-758 759-759 761-762 763-764 765-766 767-768 769-769 771-772 773-774 775-776 777-778 779-779 781-782 783-784 785-786 787-788 789-789 791-792 793-794 795-796 797-798 799-799 801-802 803-804 805-806 807-808 809-809 811-812 813-814 815-816 817-818 819-819 821-822 823-824 825-826 827-828 829-829 831-832 833-834 835-836 837-838 839-839 841-842 843-844 845-846 847-848 849-849 851-852 853-854 855-856 857-858 859-859 861-862 863-864 865-866 867-868 869-869 871-872 873-874 875-876 877-878 879-879 881-882 883-884 885-886 887-888 889-889 891-892 893-894 895-896 897-898 899-899 901-902 903-904 905-906 907-908 909-909 911-912 913-914 915-916 917-918 919-919 921-922 923-924 925-926 927-928 929-929 931-932 933-934 935-936 937-938 939-939 941-942 943-944 945-946 947-948 949-949 951-952 953-954 955-956 957-958 959-959 961-962 963-964 965-966 967-968 969-969 971-972 973-974 975-976 977-978 979-979 981-982 983-984 985-986 987-988 989-989 991-992 993-994 995-996 997-998 999-999

.....
.....
.....

THE UNITED STATES OF AMERICA, Plaintiff,
v.
JOHN T. KELLY, et al., Defendants.

וְאֵת שְׁנִי כְּלָמָדְךָ בְּבָנָךְ וְאֵת שְׁלִישִׁי כְּלָמָדְךָ בְּבָנָךְ וְאֵת

Table II

Newly identified lines of the (010-000) and (020-010) bands.

Transition	Position
<u>(010-000) band</u>	
$^{21}_{1,21} - ^{20}_{0,20}$ }	1949.9147 cm^{-1}
$^{21}_{0,21} - ^{20}_{1,20}$	
$^{22}_{1,22} - ^{21}_{0,21}$ }	1963.4065
$^{22}_{0,22} - ^{21}_{1,21}$	
$^{23}_{1,23} - ^{22}_{0,22}$ }	1976.7223
$^{23}_{0,23} - ^{22}_{1,22}$	
$^{24}_{1,24} - ^{23}_{0,23}$ }	1989.9184
$^{24}_{0,24} - ^{23}_{1,23}$	
<u>(020-010) band</u>	
$^{12}_{1,12} - ^{11}_{0,11}$	1780.9916
$^{12}_{0,12} - ^{11}_{1,11}$	1780.9407
$^{13}_{1,12} - ^{12}_{2,11}$	1849.5795
$^{13}_{1,13} - ^{12}_{0,12}$	1797.0532
$^{13}_{0,13} - ^{12}_{1,12}$	1797.0276
$^{14}_{1,13} - ^{13}_{2,12}$	1868.0298
$^{14}_{1,14} - ^{13}_{0,13}$	1812.8915
$^{14}_{0,14} - ^{13}_{1,13}$	1812.8915 blended
$^{15}_{3,13} - ^{14}_{2,12}$	1931.9649
$^{15}_{2,13} - ^{14}_{3,12}$	1928.6794
$^{15}_{2,14} - ^{14}_{1,13}$	1888.0332
$^{15}_{1,14} - ^{14}_{2,13}$	1887.7405

Table II (Continued)

Transition	Position
$15_{1,15} - 14_{0,14}$	1828.5181 cm^{-1}
$15_{0,15} - 14_{1,14}$	1828.5127
$16_{3,14} - 15_{2,13}$	1951.2771
$16_{2,15} - 15_{1,14}$	1906.3849
$16_{1,15} - 15_{2,14}$	1906.2534
$16_{1,16} - 15_{0,15}$ }	1843.9477
$16_{0,16} - 15_{1,15}$	
$17_{1,17} - 16_{0,16}$ }	1859.2010
$17_{0,17} - 16_{1,16}$	
$18_{1,18} - 17_{0,17}$ }	1874.3132
$18_{0,18} - 17_{1,17}$	
$19_{1,19} - 18_{0,18}$ }	1889.3063
$19_{0,19} - 18_{1,18}$	
$20_{1,20} - 19_{0,19}$ }	1904.2398
$20_{0,20} - 19_{1,19}$	

**DATE
ILME**